HHS Public Access

Author manuscript

J Rheol (N Y N Y). Author manuscript; available in PMC 2018 May 18.

Published in final edited form as:

J Rheol (N Y N Y). 2018 May ; 62(3): 695–712. doi:10.1122/1.4996320.

Nonlinear viscoelastic characterization of human vocal fold tissues under large-amplitude oscillatory shear (LAOS)

Roger W. Chan

Speech Language Pathology and Audiology, National Taipei University of Nursing and Health Sciences, Taipei, Taiwan

Abstract

Viscoelastic shear properties of human vocal fold tissues were previously quantified by the shear moduli (G' and G''). Yet these small-strain linear measures were unable to describe any nonlinear tissue behavior. This study attempted to characterize the nonlinear viscoelastic response of the vocal fold lamina propria under large-amplitude oscillatory shear (LAOS) with a stress decomposition approach. Human vocal fold cover and vocal ligament specimens from eight subjects were subjected to LAOS rheometric testing with a simple-shear rheometer. The empirical total stress response was decomposed into elastic and viscous stress components, based on odd-integer harmonic decomposition approach with Fourier transform. Nonlinear viscoelastic measures derived from the decomposition were plotted in Pipkin space and as rheological fingerprints to observe the onset of nonlinearity and the type of nonlinear behavior. Results showed that both the vocal fold cover and the vocal ligament experienced intercycle strain softening, intracycle strain stiffening, as well as shear thinning both intercycle and intracycle. The vocal ligament appeared to demonstrate an earlier onset of nonlinearity at phonatory frequencies, and higher sensitivity to changes in frequency and strain. In summary, the stress decomposition approach provided much better insights into the nonlinear viscoelastic behavior of the vocal fold lamina propria than the traditional linear measures.

Keywords

Larynx; nonlinear viscoelasticity; shear deformation; strain softening; strain stiffening; Pipkin diagram

I. INTRODUCTION

The human vocal fold is a layered structure composed of a stratified squamous epithelium on the medial surface, a connective tissue layer (namely lamina propria) immediately

Correspondence: Roger W. Chan, Department of Speech Language Pathology and Audiology, National Taipei University of Nursing and Health Sciences, 89 Nei Jiang Street, Taipei City, Taiwan, Republic of China 10845, Phone: +886 (2) 2822-7101 extension 6201, FAX: +886 (2) 2389-1404, waikai@ntunhs.edu.tw.

W. Chan (ORCID 0000-0002-7135-9702)

SUPPLEMENTARY MATERIAL

See online supplementary material for two appendices: Appendix A on how portions of the MITlaos MATLAB code were modified to accommodate our data sets for processing and analysis; Appendix B showing the linear viscoelastic moduli (G' and G'') for the vocal fold cover and the vocal ligament of a 53-year-old male (Subject 5) as a function of frequency (at 1.0% strain).

underneath, and a muscle layer lateral to the lamina propria [1, 2]. During voice production or phonation, the vocal folds undergo expiratory airflow-induced self-sustained oscillation to generate acoustic energy, with the epithelium and the superficial layer of the lamina propria being the major anatomical site of tissue vibration [2]. In the speech and voice science literature, this vocal fold histological structure has often been described by a body-ligament-cover model, with the vocal fold cover consisting of the epithelium and the superficial layer of the lamina propria, the vocal ligament consisting of the middle layer (or intermediate layer) and deep layer of the lamina propria, and the body consisting of the thyroarytenoid muscle [1-4].

The viscoelastic shear properties of the vocal folds are among the most important biomechanical properties for understanding phonation, as a shear wave called the "mucosal wave" propagates on the vocal fold surface during self-sustained oscillation [2]. Typically, viscoelastic shear properties of vocal fold tissues have been described by linear viscoelastic functions, specifically the elastic shear modulus G' and viscous shear modulus G'' as functions of frequency, which can be quantified by simple-shear deformation applied at small strain amplitudes when the tissue mechanical response is linear [5, 6]. In this paper, G' and G'' will be referred to as the "storage modulus" and the "loss modulus", respectively, in accordance with the nomenclature approved by the Society of Rheology.

From such linear viscoelastic measures of shear properties, i.e., storage modulus G' and loss modulus G'', both as functions of shear strain, the onset of nonlinear tissue behavior can be determined by the appearance of a downward trend in a strain sweep test (Figure 1a) [6]. According to the theory of linear viscoelasticity, these linear measures can be defined in the following constitutive equation:

$$\tau^* = G' \gamma^* + \frac{G''}{\omega} \frac{d\gamma^*}{dt} \quad (1)$$

where $\boldsymbol{\tau}^*$ is the complex shear stress, $\boldsymbol{\gamma}^*$ is the complex shear strain, t is time, and ω is the angular frequency. The definitions of the linear viscoelastic functions G' and G'' in Equation (1) are based on the assumption of linearity, with the total complex stress $\boldsymbol{\tau}^*$ being the sum of the elastic component (real part) and the viscous component (imaginary part), provided that the input signal is sinusoidal and periodic. G' and G'' can also be denoted as G'_1 and G''_1, respectively, to reflect the fact that they are the linear viscoelastic moduli of the first order (first harmonic storage modulus and loss modulus, respectively).

Once tissue behavior enters the nonlinear regime associated with large-strain amplitudes, the linear viscoelastic moduli G' and G'' can no longer sufficiently describe the nonlinear mechanical response since the nonlinear stress response is not a single-harmonic sinusoid [7, 8]. To illustrate this point, Figure 1 shows the results of strain sweep tests performed on the vocal fold lamina propria (specifically the superficial layer, or vocal fold cover) of a 60-year-old male (Subject 1), with the tissue being subjected to large-amplitude oscillatory shear (LAOS) deformation. As shown in Figure 1a, the linear measures G' and G'' can be used to illustrate the onset of nonlinear viscoelastic behavior as shown by their downward trends

with increasing strain amplitude (γ_0). These measures indicate that the linear viscoelastic regime is approximately at or below a strain level of 0.05 for this subject, where G' and G'' are independent of strain. In the nonlinear viscoelastic regime, however, rich nonlinear behavior becomes apparent in the raw stress-strain (Lissajous-Bowditch) curves, as shown by the distorted elliptical shapes of the curves with increasing strain (Figure 1b). Hence the linear, first harmonic measures are insufficient to characterize the complex nature of the nonlinear tissue behavior under LAOS. The linear measures could only indicate whether or not nonlinearity has been reached, but not the type of nonlinear behavior. Additional parameters are necessary to truly characterize the nonlinear behavior.

Here, we describe two key terms necessary for understanding the nature of nonlinear behavior under LAOS deformation: *intracycle* and *intercycle*. Intracycle refers to the mechanical behavior occurring within one stress-strain curve cycle as the strain oscillates between the minimum and the maximum imposed strain amplitude. Intercycle, on the other hand, refers to the behavior occurring across cycles of different maximum imposed strain amplitudes. Ewoldt et al. [8] developed a rheological framework for better describing such nonlinear behavior and for quantifying the mechanical response under LAOS. This framework is based on the geometric (orthogonal) stress decomposition approach with Fourier Transform processing to decompose a filtered/smoothed total stress signal (derived from the measured stress response) using only odd-integer harmonic components, with the total stress being the sum of the elastic stress and viscous stress contributions [7]. With such harmonic decomposition of the total stress response, the elastic stress component and the viscous stress component can be expressed by Chebyshev polynomials of the first kind, while nonlinear viscoelastic parameters are simultaneously derived: (1) intracycle elastic Chebyshev coefficients e_n to reflect strain stiffening/softening, (2) intracycle viscous Chebyshev coefficients v_n to reflect shear thickening/thinning, (3) instantaneous intercycle storage moduli (elastic moduli) G'_M and G'_L (G'_M for the minimum strain and G'_L for the largest strain), and (4) instantaneous intercycle coefficients of viscous dissipation (i.e., dynamic viscosities) η'_M and η'_L (η'_M for the minimum strain rate and η'_L for the largest strain rate) [8]. These nonlinear measures are summarized in Table I, and Figure 2 provides a graphic illustration of these measures. Figure 2 shows the smoothed Lissajous-Bowditch curves of the vocal fold cover of a 53-year-old male (Subject 5), illustrating the definitions of the intercycle parameters: G'_M is the tangent slope at minimum (zero) strain, G'_L is the slope of the secant at the largest (maximum) strain (Figures 2a, 2b), η'_M is the tangent slope at minimum (zero) strain rate, and η'_L is the slope of the secant at the largest strain rate (Figures 2c, 2d). The plots on the left were obtained at small strain amplitudes (1.0-2.0%) and demonstrated linear viscoelastic response, as indicated by the elliptical shapes of the elastic and viscous Lissajous-Bowditch curves (Figures 2a and 2c, respectively), whereas those on the right were obtained at 50% strain amplitude, demonstrating nonlinear response with the elliptical Lissajous-Bowditch curves distorted (Figures 2b and 2d). These curves could also provide information on the intracycle nonlinear behavior. Based on the definitions of the nonlinear viscoelastic parameters (Table I), intracycle nonlinear behavior can be determined by comparing the slopes within the Lissajous-Bowditch curves. To illustrate this, in Figure 2b the slope of the secant at maximum strain, or G'_L, is larger/steeper than the

tangent slope at zero strain, or G'_M, indicating that the vocal fold cover was experiencing intracycle strain stiffening. In Figure 2d, $\eta'_L < \eta'_M$, indicative of intracycle shear thinning.

In addition, these nonlinear parameters can be examined in an experimental test space defined by two key parameters of LAOS deformation: frequency and strain amplitude $\{\omega, \gamma_0\}$. This test space is called a Pipkin space, with ω on the x-axis and γ_0 on the y-axis, within which smoothed Lissajous-Bowditch curves can be compactly represented in a Pipkin diagram (or Pipkin space diagram) with a MATLAB program called MITlaos [8, 9]. The nonlinear viscoelastic parameters generated by MITlaos also provide a unique "rheological fingerprint" for characterizing both linear and nonlinear behavior. For our purposes, rheological fingerprints are contour plots of the nonlinear viscoelastic measures displaying their variations with $\{\omega, \gamma_0\}$ simultaneously. The nonlinear parameters can also be displayed as functions of frequency only or strain amplitude only, in order to highlight their dependence on ω alone and on γ_0 alone, in two-dimensional "scatter plots".

In the present study, this stress decomposition approach was adopted to characterize the nonlinear viscoelastic response of the vocal fold lamina propria when subjected to LAOS. In the context of phonation, the relevant physiological frequency range for vocal fold oscillatory shear is around 100-300 Hz, which is the range of average fundamental frequency of vocal fold oscillation for male and female conversational speech, with male voice towards the lower end of this range and female voice towards the higher end [2]. And the relevant physiological range of shear strain that could be achieved during large-amplitude vocal fold oscillation for loud voice production could reach around 50% [2]. Rheometric testing was performed on different layers of the lamina propria, including the vocal fold cover (superficial layer) and vocal ligament (middle and deep layers). Tissue specimens were subjected to increasing strain amplitudes of LAOS, i.e., strain sweeps at multiple frequencies. Pipkin space diagrams, rheological fingerprint plots, and scatter plots of the nonlinear viscoelastic parameters were used to characterize both the onset of nonlinear viscoelastic behavior and the nature of such behavior in the vocal fold specimens. Comparisons of nonlinear viscoelastic parameters, Pipkin space diagrams, as well as rheological fingerprints will be made for the vocal fold cover versus the vocal ligament. The comparisons of nonlinear viscoelastic parameters shown in scatter plots serve to isolate the effects of frequency and strain on nonlinear tissue behavior, whereas the Pipkin space diagrams and the rheological fingerprints serve to depict the combined influence of ω and γ_0.

II. METHOD

A. Rheometric testing of human vocal fold specimens

Four excised human larynges were obtained from the Willed Body Program of UT Southwestern Medical Center, the author's previous affiliation. Surgical specimens were also obtained from four other subjects who underwent total laryngectomy. The tissue procurement protocol and the experimental protocol were approved by the local Institutional Review Board. The characteristics of all 8 subjects are shown in Table II. Vocal fold specimens were dissected from the larynges using instruments for phonomicrosurgery as described in Chan and Rodriguez [6]. Briefly, the dissection of the vocal fold cover was

performed by making an incision on the superior surface of the vocal fold epithelium with a No. 11 surgical blade such that the vocal fold cover (which consists of the epithelium and the superficial layer of the lamina propria) could be separated from the vocal ligament through blunt dissection. After the vocal fold cover was removed, the vocal ligament (middle and deep layers of the lamina propria) was dissected by separating it from the thyroarytenoid (vocalis) muscle. The samples were kept in phosphate buffered saline solution at *p*H 7.4 at room temperature prior to rheometric testing. Oscillatory shear deformation of the specimens was performed with a frequency sweep protocol and a strain sweep protocol, using the simple-shear rheometer described previously [6] (Figure 3).

The gap between the upper plate and lower plate of the rheometer was set to be between 0.3 and 1.0 mm, such that there was complete contact between the specimen and the two tissue plates for each specimen, with the area of contact equal to or smaller than the overlapping area of the plates. The frequency sweep protocol was performed in a frequency range of 1-250 Hz, at the lowest strain amplitude (at around 1.0% to 2.0% strain). The strain sweep protocol was conducted at 100 Hz for 4 of the 8 subjects (for Subjects 1-4), and at multiple frequencies (50 Hz, 75 Hz, 100 Hz, 125 Hz, 150 Hz, 175 Hz) for the other four, over a range of displacement amplitudes of 0.004 to 1.0 mm (corresponding to a strain of around 1.0% to 50% or 100%). It was not an ideal strain sweep protocol that different levels of strain had to be applied to different tissue specimens, but different gap sizes of the rheometer had to be used to accommodate the different specimen dimensions, in order to ensure complete contact of the specimens with the tissue plates during the oscillatory shear deformation.

During rheometric testing, the samples were kept in an environmental chamber at approximately 37°C, with close to 100% relative humidity to keep the samples hydrated and to mimic physiological conditions during testing. Raw load and displacement data were collected with the WINTEST data acquisition and analysis program (EnduraTEC Systems Group, Bose Corporation, Eden Prairie, MN), at a sampling rate of 5000 samples/s. Images of the specimens were taken before each frequency sweep and strain sweep test in order to determine the area of the specimen in contact with the tissue plates, based on image analysis with NIH ImageJ (Bethesda, MD).

All tissue specimens achieved the “alternance” state or “preconditioned” state due to stress relaxation, as defined by stabilization of the cyclic stress-strain response, after an initial transient phase upon the application of the large-amplitude oscillatory shear. No discernable difference in the transient response was observed between the vocal fold cover and the vocal ligament. Both tissue types achieved the stabilized preconditioned or “alternance” state typically after about 60-100 cycles at 100 Hz, where the measured stress gradually decreased until stabilization of the mechanical response was achieved. Data were collected for the nonlinear viscoelastic measures after this stabilized state was achieved.

B. MITlaos analysis of rheometric testing data

The raw displacement and load data obtained from the WINTEST software were converted into shear strain and shear stress, respectively, based on conversion factors derived from the known rheometer gap size and the measured specimen contact area [6]. The data were also input into the MITlaos MATLAB program for the nonlinear viscoelastic characterization,

based on harmonic decomposition of the total stress response using Fourier transform. Portions of the MATLAB program were modified in order to accommodate our data sets, such as the use of a higher sampling rate (5000 samples/s) for our data when compared to that of Ewoldt et al. [8] (details of the modified code are shown in Appendix A). After the raw data were converted into stress and strain, the appropriate odd-integer harmonics for Fourier transform of the total stress response were chosen in MITlaos. The criteria for choosing the appropriate odd harmonics were that the highest odd harmonic to be selected contributed greater than 5% of the first harmonic contribution, and that the contribution of noise from the higher-order odd harmonics was minimized. Smoothed Lissajous-Bowditch plots as well as values of nonlinear viscoelastic parameters corresponding to the harmonic decomposition were generated by MITlaos, in order to characterize the nonlinear viscoelastic behavior of the human vocal fold cover and vocal ligament specimens.

III. RESULTS AND DISCUSSION

A. Nonlinear elastic and viscous measures at constant frequency

The first set of results shown are averages of the nonlinear measures derived from MITlaos for all eight subjects (Table II), at a single frequency of $\omega = 628$ rad/s (100 Hz) within the phonatory range, such that the effect of strain alone on the nonlinear viscoelastic behavior of the vocal fold cover and vocal ligament can be observed. Figure 4 compares the average intercycle elastic measures of the vocal fold cover to those of the vocal ligament. The intercycle storage moduli (elastic moduli) G'_M and G'_L were plotted against strain amplitude γ_0 for the cover (Figure 4a) and for the ligament (Figure 4b). The linear storage modulus of the first order (G'_1) was also shown for comparisons to the nonlinear measures. Note that the number of specimens (n) for each data point (with the labels “n=2”, “n=3”, “n=8”, etc.) indicated the number of subjects that was tested at that particular strain amplitude, with each specimen coming from a unique subject. The number of subjects (specimens) tested was not the same for different strain amplitudes, because the rheometer gap size was varied to ensure complete contact between the specimens and the rheometer plates, resulting in different imposed strain values for different subjects. Also note that for some of the nonlinear viscoelastic measures (in Figure 4 and in other following figures) the error bars (standard deviations) of the data points were quite large, which was likely a mix of the actual differences between the different subjects and experimental errors related to possible differences in specimen preparation (dissection) and loading in the rheometer. For readers who are interested in the linear viscoelastic response of the tissues as a function of frequency, please refer to Appendix B, which shows the linear storage and loss moduli (G'_1 and G''_1) of a 53-year-old male (Subject 5). The data showed that both the vocal fold cover and the vocal ligament could be considered as viscoelastic solids in their linear regime of deformation, consistent with our previous studies [5, 6].

The overall decreasing trend of G'_M and G'_L with increasing strain amplitude in Figure 4 indicated that both the vocal fold cover and the vocal ligament experienced intercycle strain softening. It was also apparent that for both cover and ligament the values of G'_M, G'_L, and G'_1 converged at small strain amplitudes. This indicated that the tissue mechanical behavior was within the linear regime, as the onset of nonlinear behavior was characterized by a

divergence of these values. The vocal fold cover first appeared to show nonlinear behavior at about 2.5% strain, whereas the vocal ligament first showed nonlinear behavior at about 25% strain. On average, the onset of nonlinear behavior for the ligament occurred at a higher strain than the cover.

Notice that for both the cover and the ligament, the values for the linear first harmonic storage modulus G'_1 (the shaded circles) were always in between the values of G'_M and G'_L (Figure 4), as reflective of the definition of G'_1 being the average of the two nonlinear measures. Also, it was apparent that the range of values of the intercycle storage moduli for the vocal fold cover was considerably higher than the range for the vocal ligament, especially at the lower strains. This finding of the cover being stiffer than the ligament was consistent with our previous study on their tensile elastic response [10].

From the intercycle storage moduli, the intracycle nonlinear behavior could also be determined at each strain amplitude by observing whether G'_M was larger than G'_L, or vice versa, in the nonlinear regime. In our case (Figure 4), the values diverged once the nonlinear regime was reached, with G'_L larger than G'_M at almost all strain amplitudes, indicating intracycle strain stiffening for both the cover and the ligament.

In Figure 5, the intercycle nonlinear viscoelastic parameters η'_M and η'_L were plotted against strain rate amplitude $\dot{\gamma}_0$ for the vocal fold cover (Figure 5a) and for the vocal ligament (Figure 5b). The linear dynamic viscosity of the first order (η'_1) was shown for comparisons. The patterns of these plots mirrored those in Figure 4. The overall decreasing trend with increasing strain rate amplitude indicated intercycle shear thinning. Similar to the changes of G'_M and G'_L with strain amplitude, the values of the intercycle dynamic viscosities η'_M and η'_L converged at small strain rate amplitudes, and then diverged with the onset of nonlinear behavior. The dynamic viscosities for the vocal fold cover diverged at a strain rate of approximately 15 s^{-1} (Figure 5a), whereas for the vocal ligament they diverged at a strain rate of about 150 s^{-1} (Figure 5b). The general pattern was that the onset of nonlinear behavior occurred at a higher strain rate amplitude for the ligament than for the cover. The values of the linear first harmonic dynamic viscosity η'_1 were in between the values of the nonlinear dynamic viscosities, due to its definition being the average of the nonlinear measures. Also, the range of values of the dynamic viscosities for the vocal fold cover was considerably higher than that for the vocal ligament.

Similar to the situation for intercycle storage moduli, intracycle nonlinear viscous behavior could also be determined based on comparing η'_M with η'_L at each strain rate amplitude. In the nonlinear range, η'_M was shown to be larger than η'_L at almost all strain rate amplitudes for both the cover and the ligament, indicating intracycle shear thinning. In summary, both intercycle and intracycle nonlinear behavior can be observed by the changes of nonlinear parameters with strain or strain rate, and by comparisons of G'_M with G'_L or η'_M with η'_L.

The elastic and viscous Chebyshev coefficients (e_n and v_n) are strictly nonlinear measures (for $n > 1$) that characterize only intracycle nonlinearity. Hence, when the tissue mechanical response is in the linear regime, the values of the elastic and viscous Chebyshev coefficients should be zero [8]. Once the tissue behavior enters the nonlinear regime, the Chebyshev

coefficients would become non-zero, and the sign of the coefficients would dictate the type of nonlinear behavior occurring. In Figure 6, the elastic Chebyshev coefficients are plotted against strain amplitude for the vocal fold cover (Figure 6a) and for the vocal ligament (Figure 6b). It appeared that the cover was demonstrating linear behavior until the elastic Chebyshev coefficient became non-zero at around $\gamma_0 > 0.025$. This was consistent with the divergence of the intercycle storage moduli in Figure 4a, which started at around 2.5% strain. Once the cover entered the nonlinear regime, the values of e_3/e_1 were always positive, indicative of intracycle strain stiffening. For the vocal ligament (Figure 6b), the linear regime included strains of up to around 25%, and e_3/e_1 became non-zero thereafter to signify nonlinearity. This was also consistent with the observed divergence of the intercycle storage moduli (Figure 4b). Similar to the cover, the ligament experienced intracycle strain stiffening since the values of e_3/e_1 in the nonlinear regime were almost always positive. Note that the applied strain amplitude ranged from 0.004 (0.4%) to 1.0 (100%) for many of the specimens tested, especially for the vocal fold cover (Figures 4a, 6a), where there were 8 data points with at least 4 tissue specimens at any particular strain amplitude ($n \geq 4$). This wide range of strain was necessary during the strain sweep experiments to achieve LAOS. There were three strain amplitudes with (n = 8), one strain amplitude with (n = 7), and one strain amplitude with (n = 6) (Figures 4a, 6a).

Figure 7 shows the viscous Chebyshev coefficient (v_3/v_1) plotted against strain rate amplitude. In the linear regime, v_3/v_1 was zero. Tissue behavior for the vocal fold cover seemed to enter the nonlinear regime at a strain rate of about 15.0 s^{-1}, consistent with Figure 5a; whereas for the vocal ligament, tissue behavior first became nonlinear at a strain rate of around 150 s^{-1}, also consistent with the trend in Figure 5b. In the nonlinear regime, the values of v_3/v_1 were mostly negative for both the cover and the ligament, indicative of intracycle shear thinning.

B. Nonlinear elastic and viscous measures at constant strain

In addition to showing the effect of strain on nonlinear behavior of the vocal fold cover and the vocal ligament, the effect of frequency alone on tissue behavior was also considered. The results here are the averages of the MITlaos-derived nonlinear viscoelastic measures (Table II) for the eight subjects in dependence of frequency, at either a low level of strain (1 to 2%), or at high strain (50%). Figure 8 shows the results for the intercycle storage moduli. At low strain, the tissue behavior was largely linear for both the cover (Figure 8a) and the ligament (Figure 8b), except at higher frequencies. At high strain, however, nonlinear behavior strongly dependent on frequency was observed (Figures 8c, 8d). At low strain, linear behavior was maintained until a frequency of around $\omega = 1099$ rad/s (175 Hz) (for the cover) or $\omega = 785$ rad/s (125 Hz) (for the ligament), after which G'_M, G'_L, and G'_1 diverged, indicative of the onset of nonlinearity. In contrast, at 50% strain, highly nonlinear behavior for both cover and ligament (Figures 8c, 8d) was observed at all frequencies, as the values of G'_M, G'_L, and G'_1 never converged.

A general trend also apparent in Figure 8 was that of intercycle strain softening at all frequencies, based on comparisons of the moduli between Figures 8a and 8c, and between Figures 8b and 8d. This was consistent with the trend observed in Figure 4 when the effect

of strain alone on nonlinearity was considered. One interesting finding was the switch from intracycle strain stiffening to intracycle strain softening for $\omega > 628$ rad/s (100 Hz), observed for the vocal fold cover at high strain (Figure 8c).

The effect of frequency on the intercycle dynamic viscosities η'_M and η'_L for the vocal fold cover and the vocal ligament is shown in Figures 9a and 9b, respectively. The dynamic viscosities followed the general trends of the intercycle storage moduli in Figure 8. At low strain, linearity was generally maintained until a frequency of about $\omega = 1099$ rad/s (175 Hz) for the cover, or $\omega = 785$ rad/s (125 Hz) for the ligament, following which η'_M, η'_L, and η'_1 diverged, indicating nonlinearity. Highly nonlinear behavior was apparent at high strain for both cover and ligament (Figures 9c and 9d), as η'_M, η'_L, and η'_1 never converged at any frequency.

The intercycle dynamic viscosities mostly decreased with frequency, especially for the vocal fold cover (Figures 9a, 9c), and to a lesser extent for the vocal ligament (Figures 9b, 9d). Also, the intercycle dynamic viscosities at high strain (Figures 9c, 9d) were lower than those at low strain (Figures 9a, 9b) at most frequencies, indicating intercycle shear thinning for both the cover and the ligament.

Figure 10 shows the effect of frequency on the elastic Chebyshev coefficient e_3/e_1, at low strain (1-2%) and at high strain (50%). At low strain for both the vocal fold cover and the vocal ligament (Figures 10a and 10b, respectively), the tissue behavior was linear at low frequencies as the values of e_3/e_1 were zero. At low strain, nonlinear behavior was observed starting at frequencies of around $\omega > 1099$ rad/s (175 Hz) for the cover and $\omega > 785$ rad/s (125 Hz) for the ligament. At high strain, however, no linear regime was observed for both cover and ligament (Figures 10c, 10d). This was consistent with the trends observed in Figures 8c, 8d and in Figures 9c, 9d. The values of e_3/e_1 were positive at most frequencies in the nonlinear regime for both cover and ligament at both low and high strain, indicative of intracycle strain stiffening. An interesting exception to this trend can be observed in Figure 10c, where at high strain the cover seemed to have switched from intracycle strain stiffening to intracycle strain softening at a frequency of $\omega > 628$ rad/s (100 Hz). This was similar to the interesting finding in Figure 8c.

The trends of the viscous Chebyshev coefficient (v_3/v_1) shown in Figure 11 were similar to those of the elastic Chebyshev coefficient in Figure 10. At low strain, the tissue behavior seemed to be linear at low frequencies as v_3/v_1 was zero for the cover and the ligament (Figures 11a and 11b, respectively). At higher strain, there was no linear behavior at all frequencies (Figures 11c and 11d). Intracycle shear thinning at high strain could be observed for both cover and ligament, whereas at low strain it was mostly intracycle shear thickening. Note that in Figure 11d, the value of v_3/v_1 at the highest frequency was close to zero, corresponding to the convergence of the dynamic viscosities at this very same frequency (Figure 9d).

In summary, based on the patterns of the nonlinear viscoelastic parameters and their dependence on frequency and strain, it seemed that there was generally a higher sensitivity of the parameters to changes in strain than to changes in frequency at low strain, i.e., strain

has a greater effect on nonlinear behavior at low strain. Conversely, at higher strain, the parameters seemed to be more sensitive to changes in frequency than to changes in strain, i.e., at high strain, frequency has a greater effect on nonlinear behavior, with linear behavior largely absent.

C. Elastic and viscous Lissajous-Bowditch curves in Pipkin space

Smoothed elastic and viscous Lissajous-Bowditch curves generated by MITlaos for the vocal fold cover and vocal ligament were plotted in Pipkin space, where the data can be examined at multiple frequencies and strain amplitudes simultaneously [9]. The Pipkin diagram (or Pipkin space diagram) is a useful tool to determine the onset of nonlinearity, to allow for visual inspection of distortions due to noise, and to characterize nonlinear behavior [8]. It consists of a series of smoothed/filtered Lissajous-Bowditch curves with frequency ω on the x-axis and strain amplitude γ_0 on the y-axis (Figures 12 and 13). Within each individual smoothed curve, the solid line represents the total stress, and the dashed line within the solid line represents the elastic stress contribution (for elastic Lissajou-Bowditch curves) or the viscous stress contribution (for viscous Lissajous-Bowditch curves), with the total stress being the sum of the elastic and viscous stress components [7]. In the linear regime, the elastic and viscous Lissajous-Bowditch curves would normally be elliptical in shape, as $G'_M = G'_L$ and $\eta'_M = \eta'_L$. However, once nonlinearity is reached, with the elastic stress contributions and viscous stress contributions becoming increasingly nonlinear, i.e., changes in the relative values of G'_M vs. G'_L and η'_M vs. η'_L, the curves would begin to deviate from the elliptical shape, as illustrated in Figure 2. In the nonlinear regime, the distorted elastic Lissajous-Bowditch curves would take on a cubic (or odd-degree polynomial) shape, whereas the distorted viscous Lissajous-Bowditch curves tend to show a sigmoidal shape (Figure 2). Figure 12 shows the Pipkin diagrams of the elastic and viscous Lissajous-Bowditch curves for the vocal fold cover of a representative 53-year-old male (Subject 5) (Figures 12a and 12b, respectively). It was apparent that at smaller imposed strain amplitude, the tissue behavior was in the linear regime as indicated by the elliptical shapes of the curves. As strain amplitude increased, tissue behavior gradually became nonlinear with increasingly distorted elliptical shapes of the curves.

At low frequencies ($\omega \leq 628$ rad/s or 100 Hz), the onset of nonlinearity due to the elastic stress contribution seemed to occur at around 10% strain, as shown by deviations from an elliptical shape (Figure 12a). The onset of nonlinearity due to the viscous stress contribution was also at around 10% strain (Figure 12b). For both elastic and viscous stress contributions, it was observed that as frequency increased into the phonatory range (≥100 Hz), the onset of nonlinearity seemed to occur at higher strain, e.g., onset for elastic contribution at about 50% strain at $\omega = 785$ rad/s (125 Hz) (Figure 12a) and onset for viscous contribution also at about 50% strain at 125 Hz (Figure 12b).

Figure 13 shows the elastic and viscous Pipkin diagrams for the vocal ligament of Subject 5 (Figures 13a and 13b, respectively). It was apparent that the departure from linear behavior for the elastic stress contribution was more dependent on frequency for the vocal ligament (Figure 13a). For example, at $\omega \leq 628$ rad/s (100 Hz), the onset of nonlinear behavior was at around 10% strain. However, for $\omega \geq 785$ rad/s (125 Hz), nonlinearity was significantly

influenced by frequency, with the onset of nonlinearity occurring at lower strain with increasing frequency, e.g., onset at 1.0% strain at $\omega = 1099$ rad/s (175 Hz) (Figure 13a). Similarly, for the viscous stress contribution, earlier onsets of nonlinearity were observed with increasing frequency, e.g., with an onset of 2.0 to 5.0% strain at $\omega = 785$ rad/s (125 Hz) (Figure 13b). Distortions due to noise in the Pipkin diagrams were also occasionally observed at isolated strain amplitudes and frequencies, e.g., for the elastic stress contribution at 1.0% strain at 125 Hz (Figure 13a). These were likely due to experimental measurement errors related to the lower limit of the force range for the piezoelectric sensor of the rheometer [6].

Another interesting finding from the Pipkin diagrams was that for the elastic Lissajous-Bowditch curves at most frequencies, the vocal ligament seemed to show a significant increase in maximum stress with strain, up to about 50% or 75% strain, which was consistent with a primarily elastic behavior (Figure 13). However, the vocal fold cover seemed to show a much weaker increase in maximum stress with strain, which was consistent with a more viscous or yield-like behavior (Figure 12). This distinction between the cover and the ligament in elastic versus viscous behavior was consistent with previous studies on their tensile elastic response and their linear viscoelastic response [6, 10].

Overall, the viscous Pipkin diagram for the vocal ligament showed that the viscous Lissajous-Bowditch curves seemed to be more robust than the elastic Lissajous-Bowditch curves in demonstrating the onset of nonlinearity, as there was less deviation from the elliptical shape in the curves (Figure 13b). The data also showed that for frequencies below 628 rad/s (100 Hz), the slope of the elastic stress was always positive. However, for frequencies in the phonatory range (≥100 Hz), the slope of the elastic stress became negative for some of the amplitudes and frequencies (e.g., γ_0 ≥0.1 at 175 Hz). The onset of nonlinearity seemed to be dependent on both strain and frequency, with the onset being more dependent on frequency for the ligament than for the cover, consistent with the results shown in Figures 4-11.

Based on the definitions of the nonlinear viscoelastic measures, the Pipkin diagrams can also serve to determine intracycle nonlinear behavior. For example, the tangent slope at zero strain (η'_M) was always steeper than the slope of the secant at maximum strain (η'_L) (Figure 13b). As the slopes corresponded to the magnitude of η'_M and η'_L, with $\eta'_M > \eta'_L$, the data indicated that the vocal ligament underwent intracycle shear thinning, supporting the data of the viscous Chebyshev coefficient v_3/v_1 (Figure 8b).

D. Rheological fingerprints

The elastic and viscous nonlinear measures can also been visualized in rheological fingerprints, where the data in contours can be examined at multiple frequencies and strain amplitudes simultaneously [8]. The rheological fingerprints shown here are based on the same representative 53-year-old male (Subject 5) as that for the Pipkin diagrams. Figure 14 shows the rheological fingerprints of the four elastic nonlinear measures (Figures 14a - 14d) and the four viscous measures (Figures 14e - 14h) for the vocal fold cover. In Figure 14a, as strain amplitude increased, G'_M decreased and the contours indicated intercycle strain softening, consistent with Figures 4 and 8. G'_L and G'_1 also decreased with strain,

indicating intercycle strain softening as well (Figures 14b, 14c). Note that the contours became increasingly nonlinear as strain amplitude increased, with a lesser extent of strain softening observed at around $\omega = 785$ rad/s (125 Hz).

In Figure 14d, a complex pattern was observed for the elastic Chebyshev coefficient (e_3/e_1). At low frequency ($\omega \leq 785$ rad/s or 125 Hz), as strain amplitude increased, the vocal fold cover seemed to undergo intracycle strain stiffening. However, at high frequency ($\omega \geq 785$ rad/s or 125 Hz), as strain amplitude increased, the behavior seemed to have switched to intracycle strain softening. This apparent reversal of intracycle nonlinear behavior was likely due to the slope of the elastic stress component changing from the typical cubic or odd-degree polynomial shape to a sigmoidal shape in Pipkin space at frequencies above 125 Hz, and at strain amplitudes above 50% (Figure 12a). In addition, it can be seen that in the nonlinear regime ($\gamma_0 > 0.1$), the elastic Chebyshev coefficient (e_3/e_1) decreased with increasing frequency (Figure 14d).

In Figure 14e, as strain amplitude and frequency both increased, η'_M seemed to decrease and the contours became increasingly nonlinear. Similarly, both η'_L and η'_1 decreased with strain amplitude and with frequency, with increasingly nonlinear contour shapes (Figures 14f, 14g). These contours indicated intercycle shear thinning, consistent with Figures 5 and 9. The rheological fingerprint of the viscous Chebyshev coefficient (v_3/v_1) for the vocal fold cover showed that at all frequencies, with increasing strain amplitude, the tissue behavior apparently shifted into the nonlinear regime and underwent intracycle shear thinning (Figure 14h).

The elastic and viscous rheological fingerprints for the vocal ligament of the same subject (Subject 5) are shown in Figures 15a - 15d and 15e - 15h, respectively. In Figures 15a - 15c, as strain amplitude increased, G'_M, G'_L and G'_1 decreased, similar to the nonlinear elastic measures observed for the cover. For the rheological fingerprint of the elastic Chebyshev coefficient (e_3/e_1), with increasing strain amplitude, the ligament seemed to undergo intracycle strain stiffening (Figure 15d). However, unlike the vocal fold cover, strain softening was apparently limited to a relatively small region, which interestingly was not at the highest strain nor at the highest frequency.

For the vocal ligament, η'_M, η'_L, and η'_1 first decreased with frequency and then seemed to reverse to increase with frequency once $\omega \geq 785$ rad/s or 125 Hz (Figures 15e - 15g), unlike those of the vocal fold cover which only decreased with frequency. For the rheological fingerprint of the viscous Chebyshev coefficient (v_3/v_1), at low frequency (< 100 Hz), the ligament apparently underwent intracycle shear thinning with increasing strain amplitude (Figure 15h). However, at higher frequencies, there was a limited region of shear thickening that occurred in a similar frequency and strain amplitude region as the strain softening behavior observed in Figure 15d. The rheological fingerprints for the elastic versus the viscous Chebyshev coefficients were somewhat like mirror images to one another, in terms of their reversal of behavior (Figures 15d, 15h).

IV. GENERAL DISCUSSION

Previously reported variations in the densities and distributions of extracellular matrix (ECM) components in the different layers of the vocal fold lamina propria (vocal fold cover versus vocal ligament) could provide insights into the nature of nonlinear viscoelastic behavior that was observed in the present study. The vocal fold cover, or superficial layer of the lamina propria, consists of loose fibrous proteins (primarily collagen and elastin) as well as interstitial proteins or "ground substances" (glycosaminoclycans, proteoglycans, structural glycoproteins), and is the most pliable surface tissue layer primarily responsible for vibration. The vocal ligament, or middle and deep layers of the lamina propria, is rich in both elastin and collagenous fibers, especially type I and type III collagen [4, 11, 12]. The deep layer, in particular, has a high density of well-organized collagen I and III fibers, which partially penetrate into the vocalis muscle (medial portion of the thyroarytenoid muscle) [12]. The collagen and elastin within the middle and deep layers of the lamina propria combine to provide the vocal ligament the capability to withstand the tensile stress associated with vocal fold elongation during phonation [4, 10]. For the interstitial proteins, one of the most important is hyaluronic acid (HA), which is abundantly distributed throughout the lamina propria. It regulates water content of the ECM and contributes to tissue viscosity as well as shock absorption during tissue vibration [3, 13, 14]. Differences in the nonlinear elastic and viscous measures found between the vocal fold cover and the vocal ligament could be related to differences in densities and distributions of ECM components across the lamina propria layers. For instance, they could help explain the nonlinear behavior observed for the vocal fold cover and the vocal ligament (Figures 4-11). It was observed that the vocal fold cover experienced an earlier onset of nonlinear behavior when compared to the vocal ligament, but it was less sensitive to changes in frequency and strain, as shown in Pipkin diagrams of the vocal fold cover (Figure 12) versus the vocal ligament (Figure 13). For the vocal fold cover, the onset of nonlinearity seemed to be delayed at higher frequencies within the phonatory range (≥100 Hz), whereas for the vocal ligament, the onset of nonlinearity seemed to occur at a lower strain at frequencies of phonation. This greater susceptibility of the ligament to nonlinear behavior at phonatory frequencies can also be observed by comparing the mean deviations of the intracycle elastic and viscous Chebyshev coefficients (e_3/e_1, v_3/v_1) from zero between the cover and the ligament at frequencies of phonation (≥100 Hz). Figure 10 shows that the mean deviations of e_3/e_1 from zero for the ligament was about 3 times higher than for the cover at low strain, and about 4 times higher at high strain, whereas Figure 11 shows that the mean deviations of v_3/v_1 from zero for the ligament was about 5 times higher than for the cover at low strain, and about 1.5 times higher at high strain. Such nonlinear behavior of the vocal ligament could be related to its anisotropic mechanical behavior that has been empirically observed [15]. Such anisotropy is related to the microstructure of the ligament, with higher levels of collagen and elastin primarily aligned along the direction of the vocal fold found in the deep layer of the lamina propria [3, 4, 12]. Another factor is the relative densities of HA in the different layers. The middle and deep layers of the lamina propria, i.e., the vocal ligament, have been found to have abundant HA when compared to the vocal fold cover [14]. Chan et al. [16] showed that upon the enzymatic removal of HA and other glycosaminoglycans from the cover, the tissue dynamic viscosity increased by 70% at higher frequencies. This could help explain the lower

dynamic viscosities observed for the ligament (Figures 5b, 9b, 9d, and 15e to 15g) as compared to the cover (Figures 5a, 9a, 9c, and 14e to 14g), as a higher level of HA in the ligament could result in a lower tissue viscosity relative to the cover. An abundant presence of HA in the vocal ligament could help maintain an optimal tissue viscosity for facilitating phonation [16].

As illustrated by the elastic Lissajous-Bowditch curves in the Pipkin diagrams, the primarily elastic behavior of the vocal ligament over a broad range of strain (Figure 13) and the more viscous or yield-like behavior of the vocal fold cover with increasing strain (Figure 12) was likely related to the differences in densities and distributions of the ECM proteins in the cover versus in the ligament. As the fibrous proteins collagen and elastin are primarily aligned along the direction of the vocal fold in the deeper layers of the lamina propria (i.e., the ligament), they could contribute to a more elastic behavior [3, 4, 12]; whereas the more randomly aligned fibrous proteins and interstitial proteins in the superficial layer of the lamina propria (i.e., the cover) could help create a more viscous-like behavior, especially with an abundant presence of HA in the vocal fold cover [16].

Analysis of the viscoelastic behavior reported for other biological materials when subjected to LAOS may give further insights into the type of intercycle and intracycle nonlinear behavior observed for the vocal fold cover and the vocal ligament. Ewoldt et al. [17] reported the nonlinear viscoelastic properties of terrestrial slug mucus, also known as pedal mucus. The pedal mucus is a crosslinked gel of high-molecular-weight protein-polysaccharide complexes, whose properties are like those of vertebrate glycoproteins and glycosaminoglycans. It was shown that the pedal mucus was a yield stress material, becoming more fluid-like under high shear stress, i.e., shear thinning. The pedal mucus with properties like glycosaminoglycans can possibly be compared to HA and other interstitial proteins in the vocal fold lamina propria. While there is a clear distinction between vertebrate glycoproteins and glycosaminoglycans, in invertebrates this distinction is blurred [17]. It was observed that both the cover and the ligament underwent intercycle as well as intracycle shear thinning, particularly at high strain (Figures 9, 11). Given the importance of HA to tissue viscosity [3, 16], it can be postulated that just as the pedal mucus underwent shear thinning under high shear stress, HA contributed to the shear thinning effect that can facilitate phonation. Ewoldt et al. also determined that the pedal mucus underwent intracycle strain stiffening in the nonlinear regime, and that G'_M underwent strain softening as strain amplitude increased. The intracycle strain stiffening likely resulted from the extension (tensile stretch) of the pedal mucus components, i.e., stretch-stiffening, whereas the intercycle strain softening was likely related to the temporary disruption in inter-molecular bonds with increasing strain [17]. Similar findings were also reported for hagfish slime, consisting of mucin-like molecules that elongate as well as fibrous proteins that are tightly packed and aligned intermediate filaments [18]. Like the pedal mucus and the hagfish slime, both the cover and the ligament underwent intracycle strain stiffening, which could likewise be related to stretch-stiffening of the ECM proteins. The cover and ligament also underwent intercycle strain softening as strain amplitude increased, which could as well be related to disruptions in inter-molecular bonds and/or crosslinks among the ECM components.

As for the rheological fingerprints (Figures 14, 15), it was clear that the complexity of the numerous changes in contours of the viscoelastic parameters in regions of high strain and high frequency would require further investigations, especially for the contours of the elastic and viscous Chebyshev coefficients. On the other hand, the simultaneous effects of frequency and strain on tissue behavior could be visualized beyond what was already shown in the two-dimensional scatter plots (Figures 4-11). For the intercycle storage moduli of the vocal fold cover (Figures 14a - 14c), there was apparently little dependence of the intercycle strain softening on frequency (other than a drop in the extent of softening at around 785 rad/s or 125 Hz), whereas for the vocal ligament the frequency dependence was much more pronounced, as reflected by the near absence of strain softening at high frequencies (≥125 Hz) (Figures 15a - 15c). For the elastic Chebyshev coefficient of the cover (Figure 14d), there was also little frequency effect on the contours except in the high-strain region ($\gamma_0 >$ 0.1), where e_3/e_1 decreased with frequency. However, for the ligament there was a trend of stiffening with frequency at low strain and yet softening with frequency at high strain (Figure 15d). These differences in frequency effects observed for the vocal fold cover versus the vocal ligament were consistent with those revealed in Pipkin space (Figures 12 and 13), and could be related to the differences in distributions and orientations of collagen and elastin across the lamina propria, as higher levels of collagen and elastin that are better aligned in the ligament may contribute to a more rate-dependent nonlinear tissue behavior. The relative lack of a loading rate effect for the cover could be related to its relatively isotropic tissue microstructure, with relatively fewer and more randomly aligned fibrous proteins.

Age-related and gender-related changes in the expressions of ECM components of the vocal fold lamina propria could also contribute to differences in the nonlinear viscoelastic behavior of the vocal fold. For example, there have been reports on age-related decrease in elastin density in the superficial and middle layers of the lamina propria [19, 20], age-related increase in collagen throughout the lamina propria [20], higher levels of HA observed in the female vocal fold compared with male, especially for the deeper layers of the lamina propria [13, 14], and higher levels of collagen in male than in female for both the cover and the ligament [10, 21]. The microstructural distribution and alignment of collagen fibers in the lamina propria and how they could be affected by smoking has also been investigated [22]. In the current study, the tissue specimens were obtained from subjects of different age, gender, and smoking history, all of which likely influenced their viscoelastic response under LAOS. As shown in some of our previous studies on the linear viscoelastic properties of the vocal fold cover and the vocal ligament, different samples from different subjects may show somewhat different magnitudes of the storage and loss moduli as affected by factors such as age, gender, and smoking [5, 6, 22]. Such inter-subject differences in viscoelastic properties of the vocal folds have also been observed in other studies [23]. Nonetheless, to accurately discern the effects of such factors on the critical strain amplitude for the onset of nonlinearity, and on other linear and nonlinear tissue behavior would require well-designed rheological tests focusing specifically on these factors, with enough number of samples in each condition to ensure adequate statistical power. Due to the relatively small number of subjects tested in the current study, these inter-subject differences and the interesting,

important effects related to changes in ECM protein densities, distributions and alignment will have to be investigated in future studies focusing on such effects.

A better understanding of the nonlinear viscoelastic behavior of the vocal fold lamina propria under LAOS is also critical for the design and fabrication of tissue replacement materials for laryngeal tissue engineering applications. Various types of biological materials and biomimetic scaffolds have been proposed as candidates of tissue substitutes for vocal fold reconstruction involving surgical repair of lamina propria deficits, including scarring, fibrosis, tissue loss and atrophy. Such materials have included biologic ECM scaffolds, HA hydrogels, as well as aligned biomimetic scaffolds being identified as promising implants for vocal fold repair [24-27]. A better characterization of their nonlinear viscoelastic properties under LAOS in comparison with those of the vocal fold cover and vocal ligament would allow for optimized functional biomechanical and vibratory performance of the tissue substitutes during phonation.

V. CONCLUSION

A stress decomposition approach was adopted to characterize the nonlinear viscoelastic response of the human vocal fold lamina propria. Vocal fold cover and vocal ligament specimens were subjected to large-amplitude oscillatory shear (LAOS) at multiple strain amplitudes and frequencies. Results showed that both the vocal fold cover and the vocal ligament apparently demonstrated highly nonlinear viscoelastic behavior, including intercycle strain softening (decrease of the storage moduli G'_M and G'_L with strain amplitude), intracycle strain stiffening (elastic Chebyshev coefficient e_3/e_1 being positive), intercycle shear thinning (decrease of the dynamic viscosities η'_M and η'_L with strain rate amplitude), as well as intracycle shear thinning (viscous Chebyshev coefficient v_3/v_1 being negative). The vocal fold cover and the vocal ligament seemed to differ in their nonlinear response to changes in frequency and in strain amplitude. The ligament showed an earlier onset of nonlinear behavior at frequencies of phonation (≥100 Hz), and was more frequency dependent when compared to the vocal fold cover. The onset of nonlinearity occurred at higher strain for the cover at phonatory frequencies. In summary, the current approach revealed very rich nonlinear behavior for both the vocal fold cover and the vocal ligament that could not be readily captured and sufficiently described by the linear viscoelastic measures, such as G' and G''.

In the context of phonation, these findings suggested that the vocal fold cover could be especially well suited for vibration in the phonatory frequency range (about 100-300 Hz during speaking voice production). The relatively late onset of nonlinearity (at higher strain) at phonatory frequencies and the relative insensitivity to changes in frequency and strain may allow for an extended linear range of tissue behavior that would facilitate stable mucosal wave propagation before vibration becomes increasingly nonlinear. The apparent interesting switch observed for the vocal fold cover from intracycle strain stiffening to intracycle strain softening at phonatory frequencies (≥100 Hz) (Figures 8c and 10c) could also be related to phonatory needs, as the tissue viscoelastic behavior apparently changed with transitions between linearity and nonlinearity, between subphonatory and phonatory frequencies, or even perhaps between different vocal registers.

The current study demonstrated that the stress decomposition approach with MITlaos provided a proper tool to comprehensively characterize the nonlinear viscoelastic properties of human vocal fold tissues under large-amplitude oscillatory shear. Nonetheless, our observations and findings were preliminary in nature due to the limited number of tissue specimens examined, and should be corroborated by further studies with more specimens, and experiments designed for testing the effects of important factors such as age, gender, race, and pathology.

Supplementary Material

Refer to Web version on PubMed Central for supplementary material.

Acknowledgments

This study was supported by the National Institutes of Health, Grant R01 DC006101. The author would like to thank Dr. Randy Ewoldt of the University of Illinois for generously sharing the MATLAB code of the MITlaos program with us. The contributions of Elhum Naseri and Mindu Du to the empirical experiments and to drafting of a previous version of the manuscript are gratefully acknowledged.

References

1. Hirano M. Phonosurgery: basic and clinical investigations. Otologia (Fukuoka). 1975; 21:239–440.
2. Titze, IR. The myoelastic-aerodynamic theory of phonation. National Center for Voice and Speech; Salt Lake City, Utah: 2006.
3. Gray SD, Titze IR, Chan R, Hammond TH. Vocal fold proteoglycans and their influence on biomechanics. Laryngoscope. 1999; 109:845–854. [PubMed: 10369269]
4. Gray SD, Titze IR, Alipour F, Hammond TH. Biomechanical and histologic observations of vocal fold fibrous proteins. Ann Otol Rhinol Laryngol. 2000; 109:77–85. [PubMed: 10651418]
5. Chan RW, Titze IR. Viscoelastic shear properties of human vocal fold mucosa: Measurement methodology and empirical results. J Acoust Soc Am. 1999; 106:2008–2021. [PubMed: 10530024]
6. Chan RW, Rodriguez ML. A simple-shear rheometer for linear viscoelastic characterization of vocal fold tissues at phonatory frequencies. J Acoust Soc Am. 2008; 124:1207–1219. [PubMed: 18681608]
7. Cho KS, Hyun K, Ahn KH, Lee SJ. A geometrical interpretation of large amplitude oscillatory shear response. J Rheol. 2005; 49:747–758.
8. Ewoldt RH, Hosoi AE, McKinley GH. New measures for characterizing nonlinear viscoelasticity in large amplitude oscillatory shear. J Rheol. 2008; 52:1427–1458.
9. Pipkin, AC. Lectures on viscoelasticity theory. Springer; New York: 1972.
10. Chan RW, Fu M, Young L, Tirunagari N. Relative contributions of collagen and elastin to elasticity of the vocal fold under tension. Ann Biomed Eng. 2007; 35:1471–1483. [PubMed: 17453348]
11. Buhler RB, Sennes LU, Tsuji DH, Mauad T, da Silva LF, Saldiva PN. Collagen type I, collagen type III, and versican in vocal fold lamina propria. Arch Otolaryngol Head Neck Surg. 2011; 137:604–608. [PubMed: 21690513]
12. Prades JM, Dumollard JM, Duband S, Timoshenko A, Richard C, Dubois MD, Martin C, Peoc'h M. Lamina propria of the human vocal fold: histomorphometric study of collagen fibers. Surg Radiol Anat. 2010; 32:377–382. [PubMed: 19841851]
13. Butler JE, Hammond TH, Gray SD. Gender-related differences of hyaluronic acid distribution in the human vocal fold. Laryngoscope. 2001; 111:907–911. [PubMed: 11359176]
14. Lebl MD, Martins JR, Nader HB, Simoes MJ, De Biase N. Concentration and distribution of hyaluronic acid in human vocal folds. Laryngoscope. 2007; 117:595–599. [PubMed: 17415127]

15. Kelleher JE, Siegmund T, Du M, Naseri E, Chan RW. Empirical measurements of biomechanical anisotropy of the human vocal fold lamina propria. Biomech Model Mechanobiol. 2013; 12:555–567. [PubMed: 22886592]
16. Chan RW, Gray SD, Titze IR. The importance of hyaluronic acid in vocal fold biomechanics. Otolaryngol Head Neck Surg. 2001; 124:607–614. [PubMed: 11391249]
17. Ewoldt RH, Hosoi AE, McKinley GH. Nonlinear viscoelastic biomaterials: meaningful characterization and engineering inspiration. Integr Comp Biol. 2009; 49:40–50. [PubMed: 21669845]
18. Ewoldt RH, Winegard TM, Fudge DS. Nonlinear viscoelasticity of hagfish slime. Int J Nonlinear Mech. 2011; 46:627–636.
19. Moore J, Thibeault S. Insights into the role of elastin in vocal fold health and disease. J Voice. 2012; 26:269–275. [PubMed: 21708449]
20. Roberts T, Morton R, Al-Ali S. Microstructure of the vocal fold in elderly humans. Clin Anat. 2011; 24:544–551. [PubMed: 21647958]
21. Hammond TH, Gray SD, Butler JE. Age- and gender-related collagen distribution in human vocal folds. Ann Otol Rhinol Laryngol. 2000; 109:913–920. [PubMed: 11051431]
22. Kelleher JE, Siegmund T, Chan RW. Collagen microstructure in the vocal ligament: initial results on the potential effects of smoking. Laryngoscope. 2014; 124:E361–E367. [PubMed: 24473992]
23. Dion GR, Jeswani S, Roof S, Fritz M, Coelho PG, Sobieraj M, Amin MR, Branski RC. Functional assessment of the ex vivo vocal folds through biomechanical testing: A review. Mater Sci Eng C Mater Biol Appl. 2016; 64:444–453. [PubMed: 27127075]
24. Xu CC, Chan RW, Weinberger DG, Efune G, Pawlowski KS. Controlled release of hepatocyte growth factor from a bovine acellular scaffold for vocal fold reconstruction. J Biomed Mater Res A. 2010; 93:1335–1347. [PubMed: 19876951]
25. Kazemirad S, Heris HK, Mongeau L. Viscoelasticity of hyaluronic acid-gelatin hydrogels for vocal fold tissue engineering. J Biomed Mater Res B Appl Biomater. 2016; 104:283–290. [PubMed: 25728914]
26. Hughes LA, Gaston J, McAlindon K, Woodhouse KA, Thibeault SL. Electrospun fiber constructs for vocal fold tissue engineering: effects of alignment and elastomeric polypeptide coating. Acta Biomater. 2015; 13:111–120. [PubMed: 25462850]
27. Li L, Stiadle JM, Lau HK, Zerdoum AB, Jia X, Thibeault SL, Kiick KL. Tissue engineering-based therapeutic strategies for vocal fold repair and regeneration. Biomaterials. 2016; 108:91–110. [PubMed: 27619243]

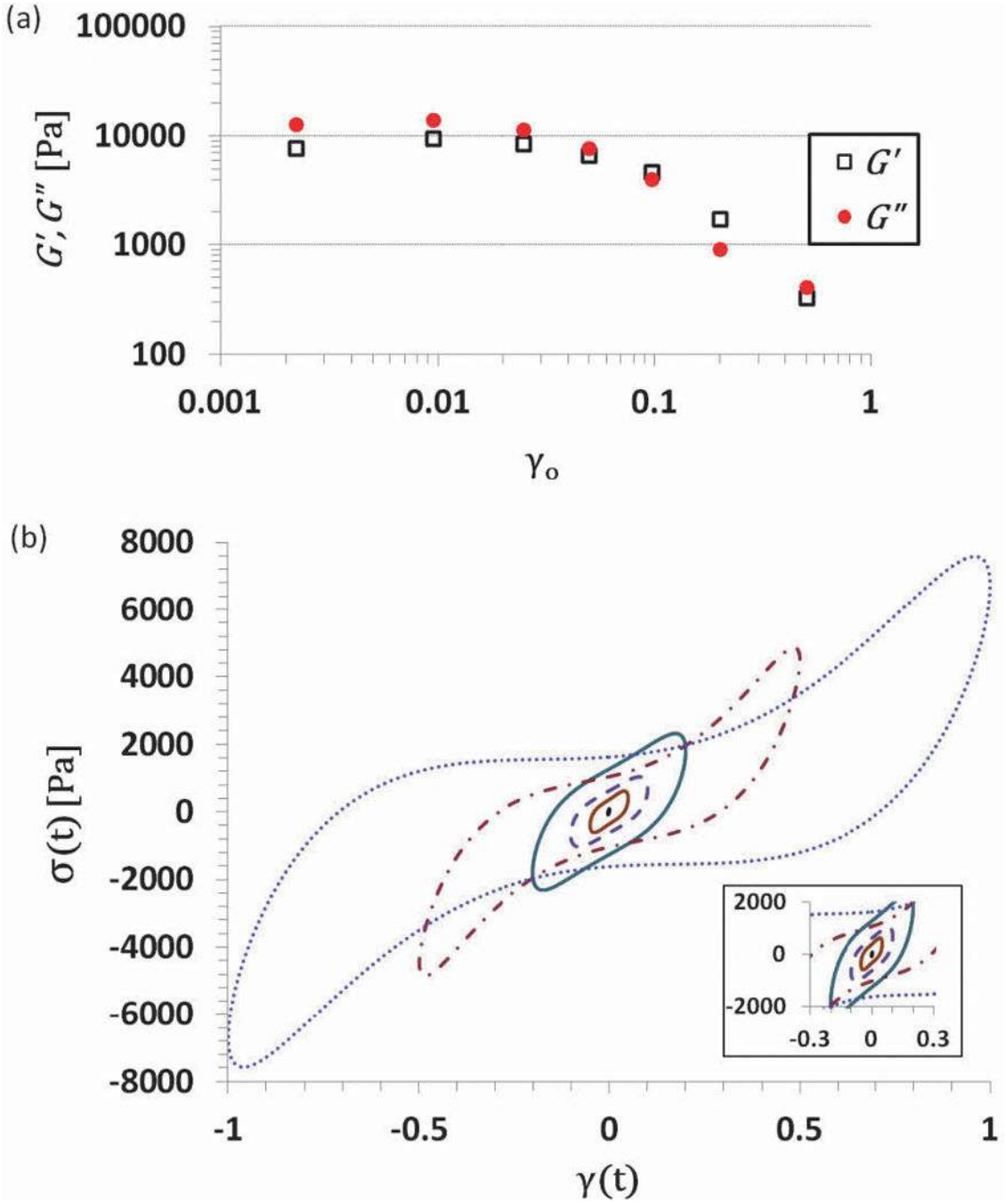

Figure 1.

Oscillatory strain sweeps of the vocal fold cover of a 60-year-old male (Subject 1) at a frequency of $\omega = 471$ rad/s (75 Hz). (a) Linear viscoelastic measures G' and G'' indicated the onset of the nonlinear regime at a strain amplitude of approximately $\gamma_0 = 0.05$. (b) Raw stress-strain data revealed rich nonlinear behavior not fully described by the traditional linear measures, particularly at high strain.

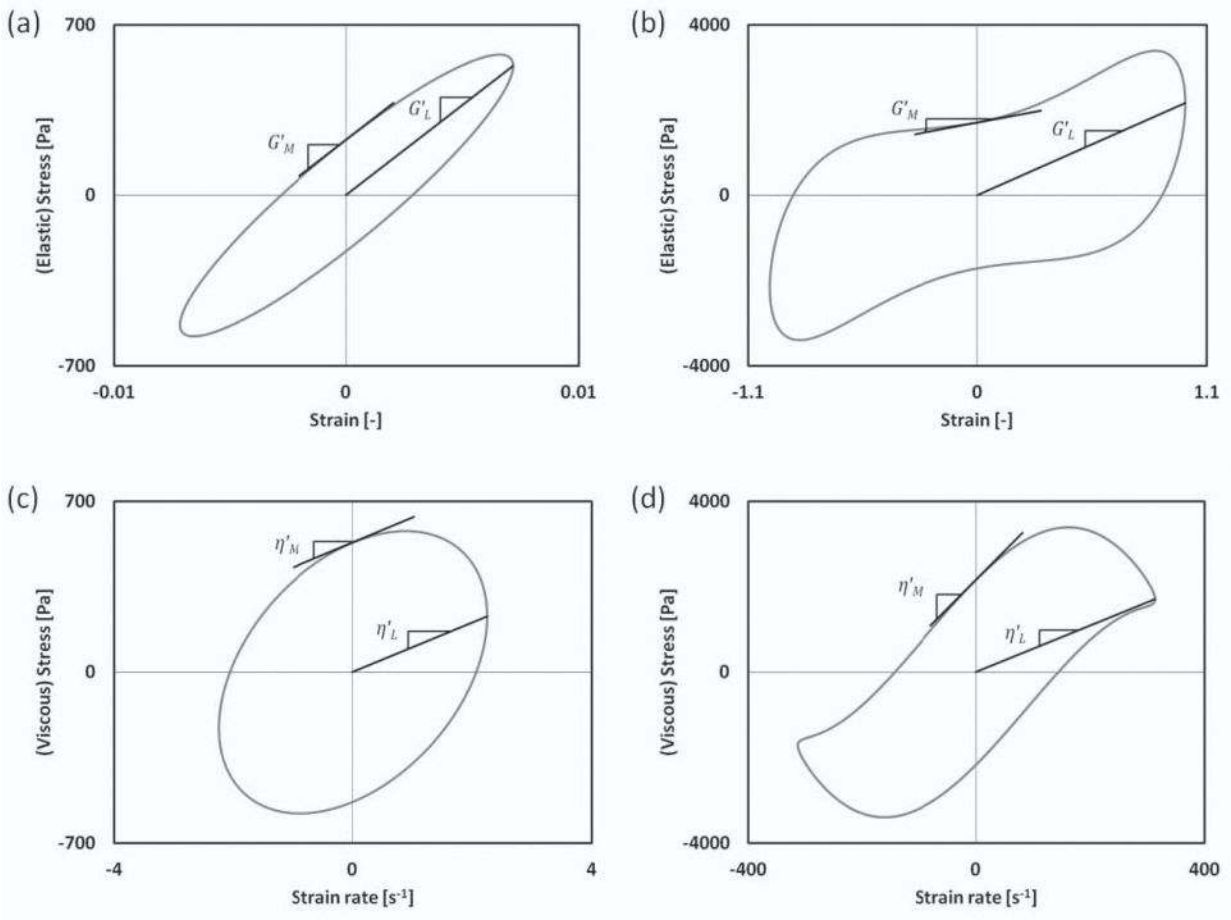

Figure 2.

Definitions of the nonlinear viscoelastic measures under large-amplitude oscillatory shear deformation, according to Ewoldt et al. [8]. The storage moduli (elastic moduli) and dynamic viscosities are defined in the Lissajous-Bowditch curves for the vocal fold cover of a 53-year-old male (Subject 5): (a) elastic Lissajous-Bowditch curve at $\omega = 942$ rad/s and $\gamma_0 = 0.02$; (b) elastic Lissajous-Bowditch curve at $\omega = 628$ rad/s and $\gamma_0 = 0.5$; (c) viscous Lissajous-Bowditch curve at $\omega = 314$ rad/s and $\gamma_0 = 0.01$; (d) viscous Lissajous-Bowditch curve at $\omega = 1099$ rad/s and $\gamma_0 = 0.5$. Undistorted elliptical shapes of the curves in (a) and (c) indicate linear viscoelastic response, whereas the distorted ellipses in (b) and (d) indicate nonlinear viscoelastic response.

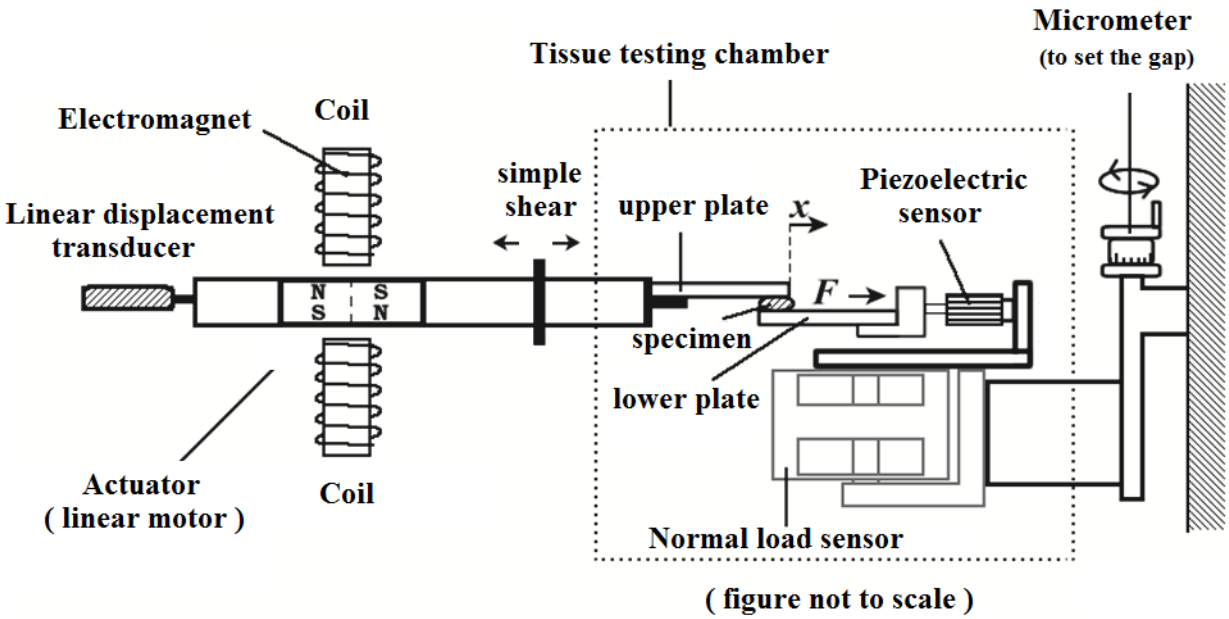

Figure 3.
Principle of the simple-shear rheometer used for large-amplitude oscillatory shear deformation, modified from Chan and Rodriguez [6].

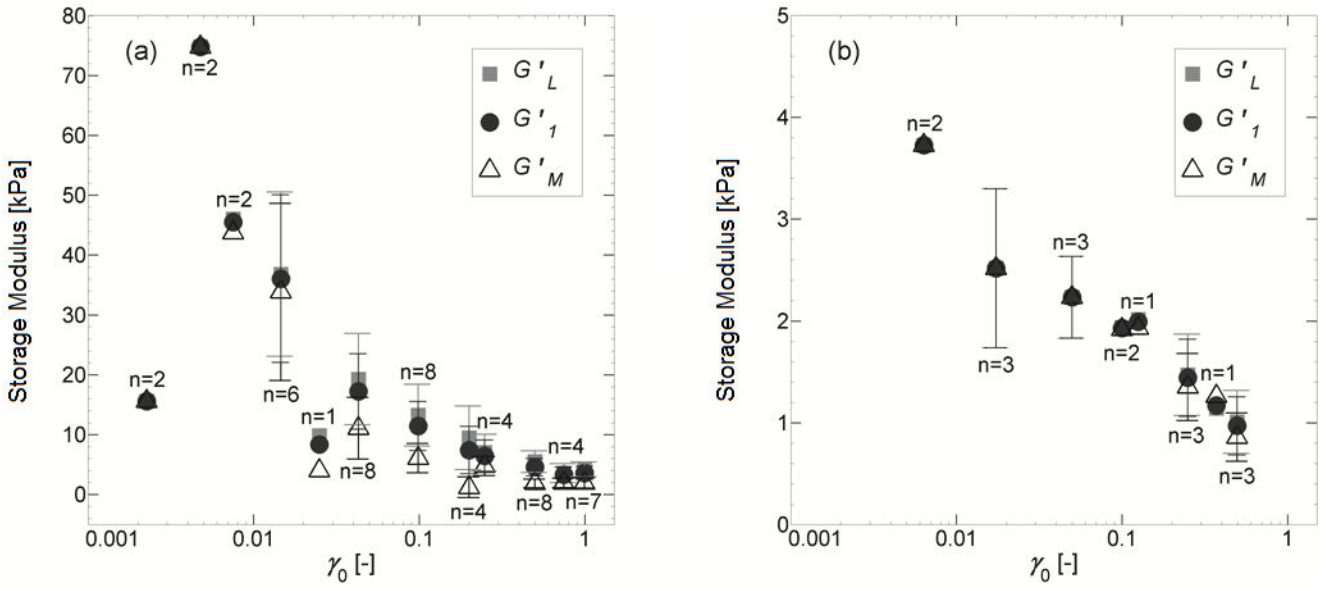

Figure 4.

Intercycle storage moduli (G'_M, G'_L, G'_1) of (a) vocal fold cover and (b) vocal ligament as a function of strain amplitude (means and standard deviations for Subjects 1-8 at 100 Hz).

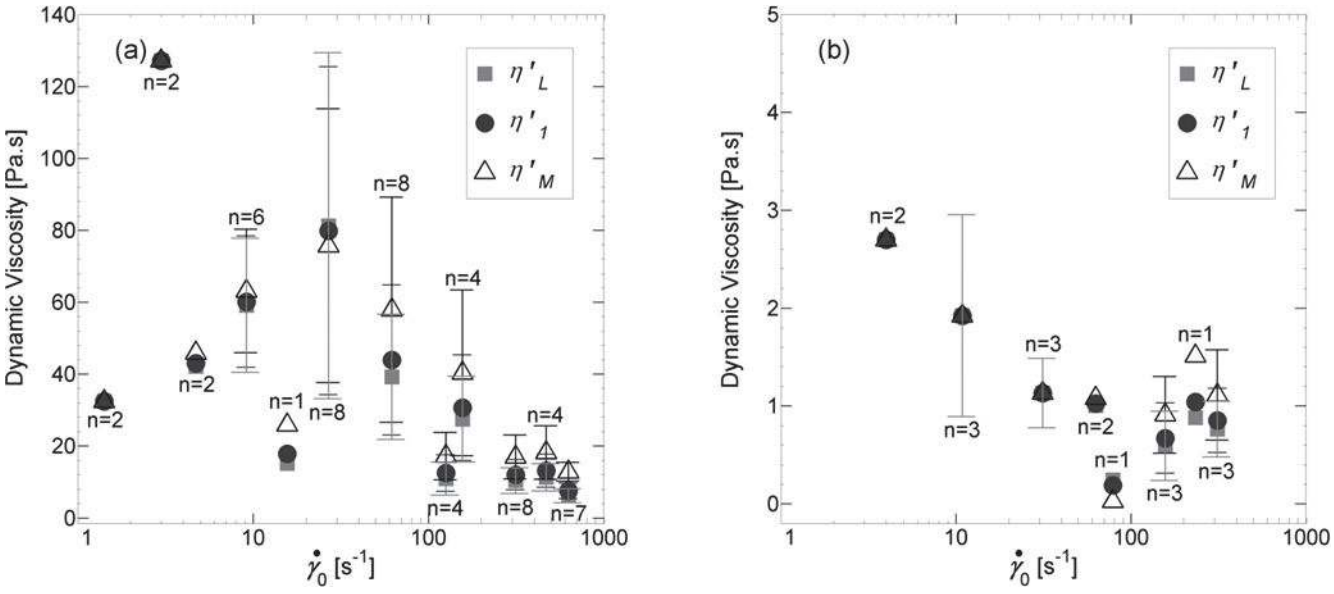

Figure 5.

Intercycle dynamic viscosities (η'_M, η'_L, η'_1) of (a) vocal fold cover and (b) vocal ligament as a function of strain rate amplitude (means and standard deviations for Subjects 1-8 at 100 Hz).

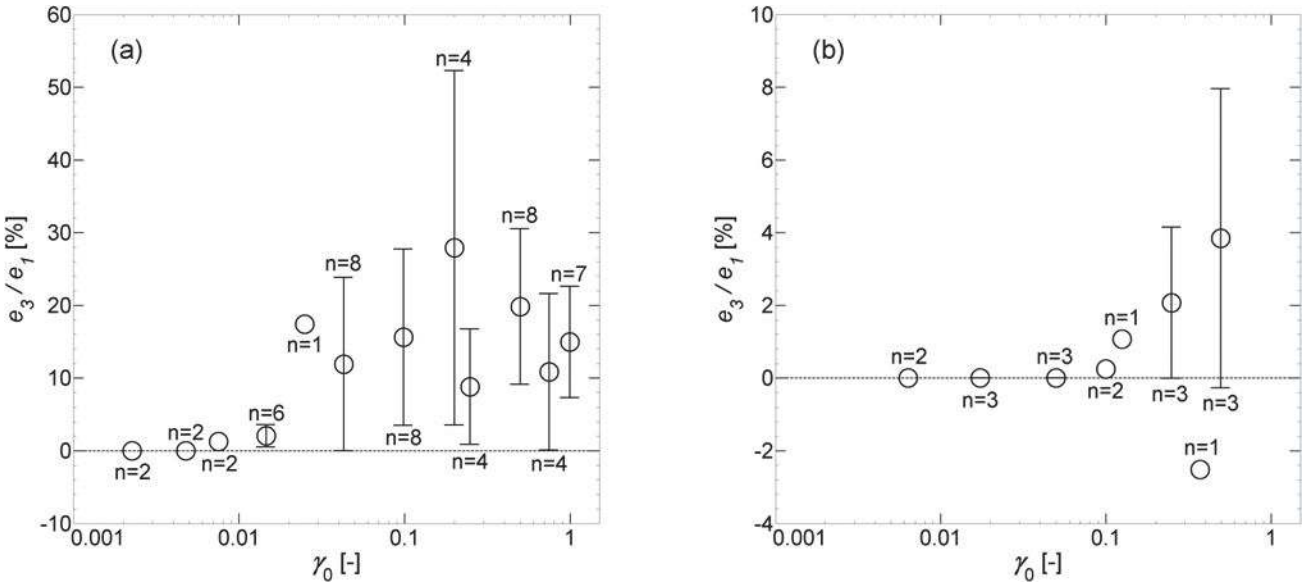

Figure 6.

Intracycle elastic Chebyshev coefficient (e_3/e_1) of (a) vocal fold cover and (b) vocal ligament as a function of strain amplitude (means and standard deviations for Subjects 1-8 at 100 Hz).

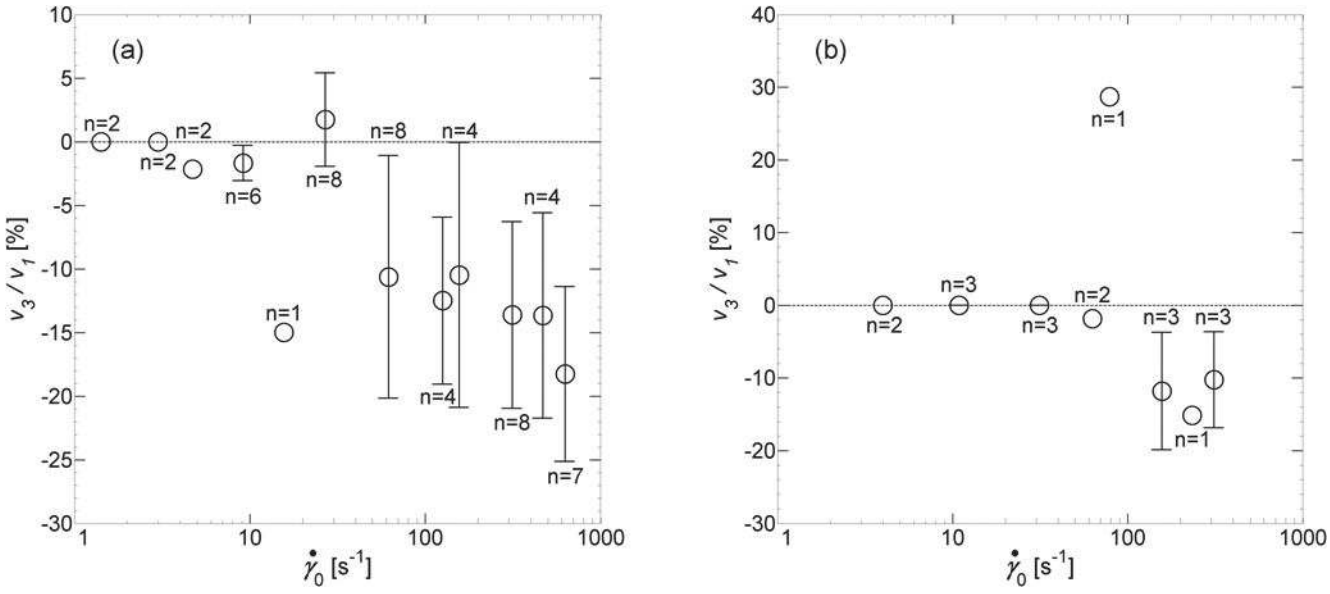

Figure 7.

Intracycle viscous Chebyshev coefficient (v_3/v_1) of (a) vocal fold cover and (b) vocal ligament as a function of strain rate amplitude (means and standard deviations for Subjects 1-8 at 100 Hz).

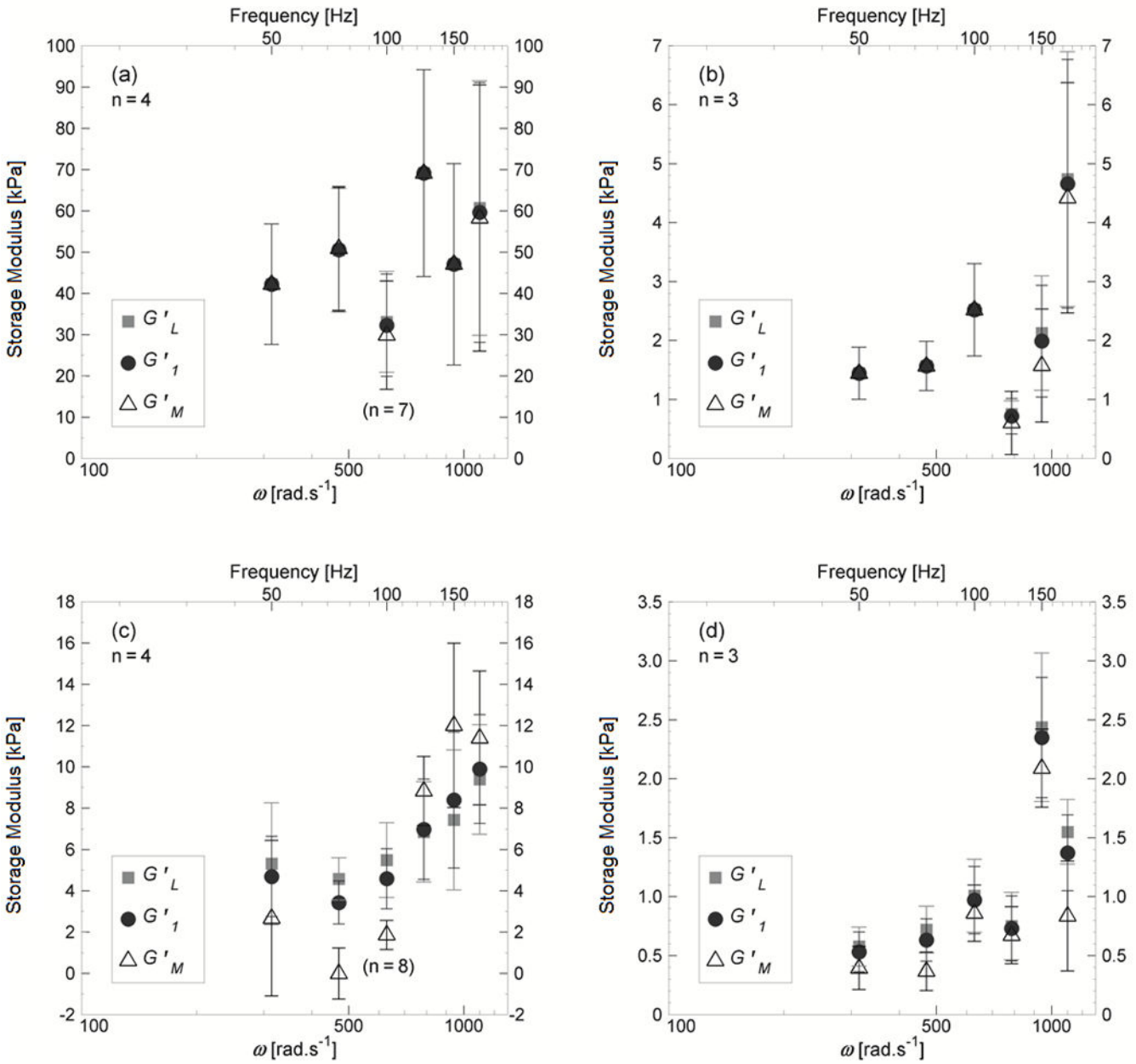

Figure 8.

Intercycle storage moduli (G'_M, G'_L, G'_1) of vocal fold cover (a, c) and vocal ligament (b, d) as a function of frequency at low strain (1-2%) (a, b) and at high strain (50%) (c, d). Shown are the averages of the elastic moduli for Subjects 1-8 (sample sizes shown in the upper left corner, except for the vocal fold cover at 100 Hz, where the sample size is indicated in parenthesis).

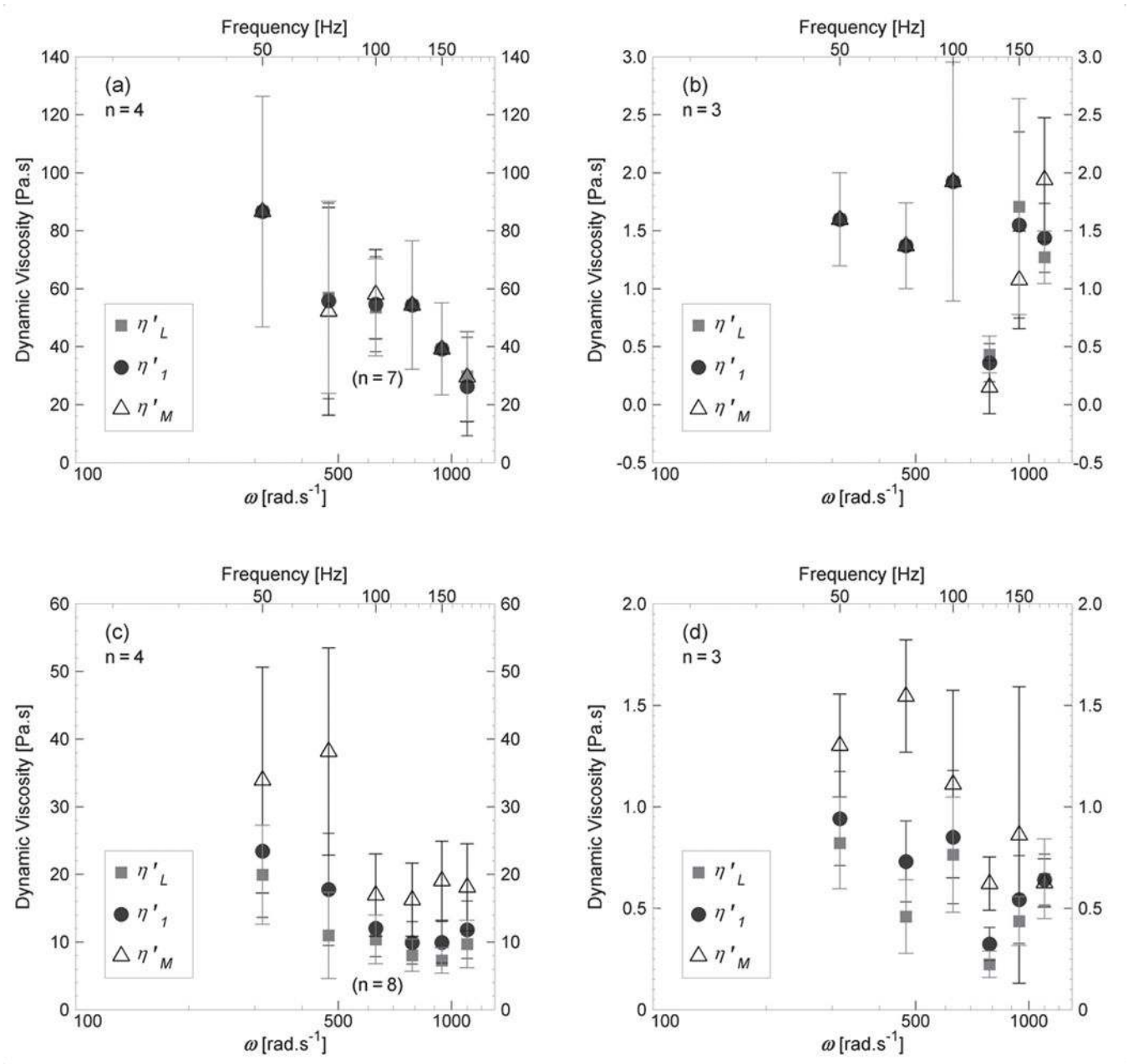

Figure 9.

Intercycle dynamic viscosities (η'_M, η'_L, η'_1) of vocal fold cover (a, c) and vocal ligament (b, d) as a function of frequency at low strain (1-2%) (a, b) and at high strain (50%) (c, d). Shown are the averages of the dynamic viscosities for Subjects 1-8 (sample sizes shown in the upper left corner, except for the vocal fold cover at 100 Hz, where the sample size is indicated in parenthesis).

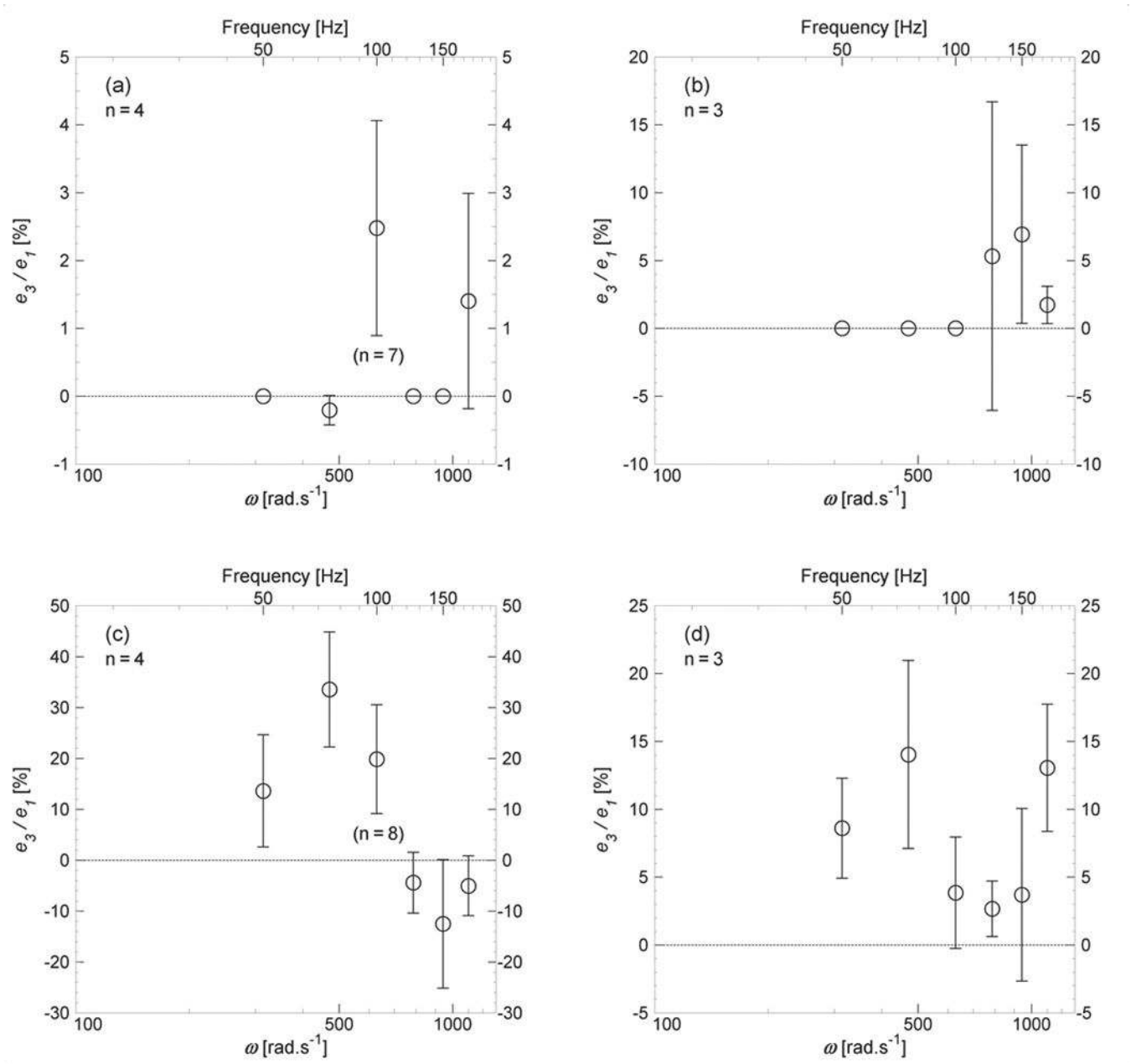

Figure 10.

Intracycle elastic Chebyshev coefficient (e_3/e_1) of vocal fold cover (a, c) and vocal ligament (b, d) as a function of frequency at low strain (1-2%) (a, b) and at high strain (50%) (c, d). Shown are the averages of the elastic Chebyshev coefficient for Subjects 1-8 (sample sizes shown in the upper left corner, except for the vocal fold cover at 100 Hz, where the sample size is indicated in parenthesis).

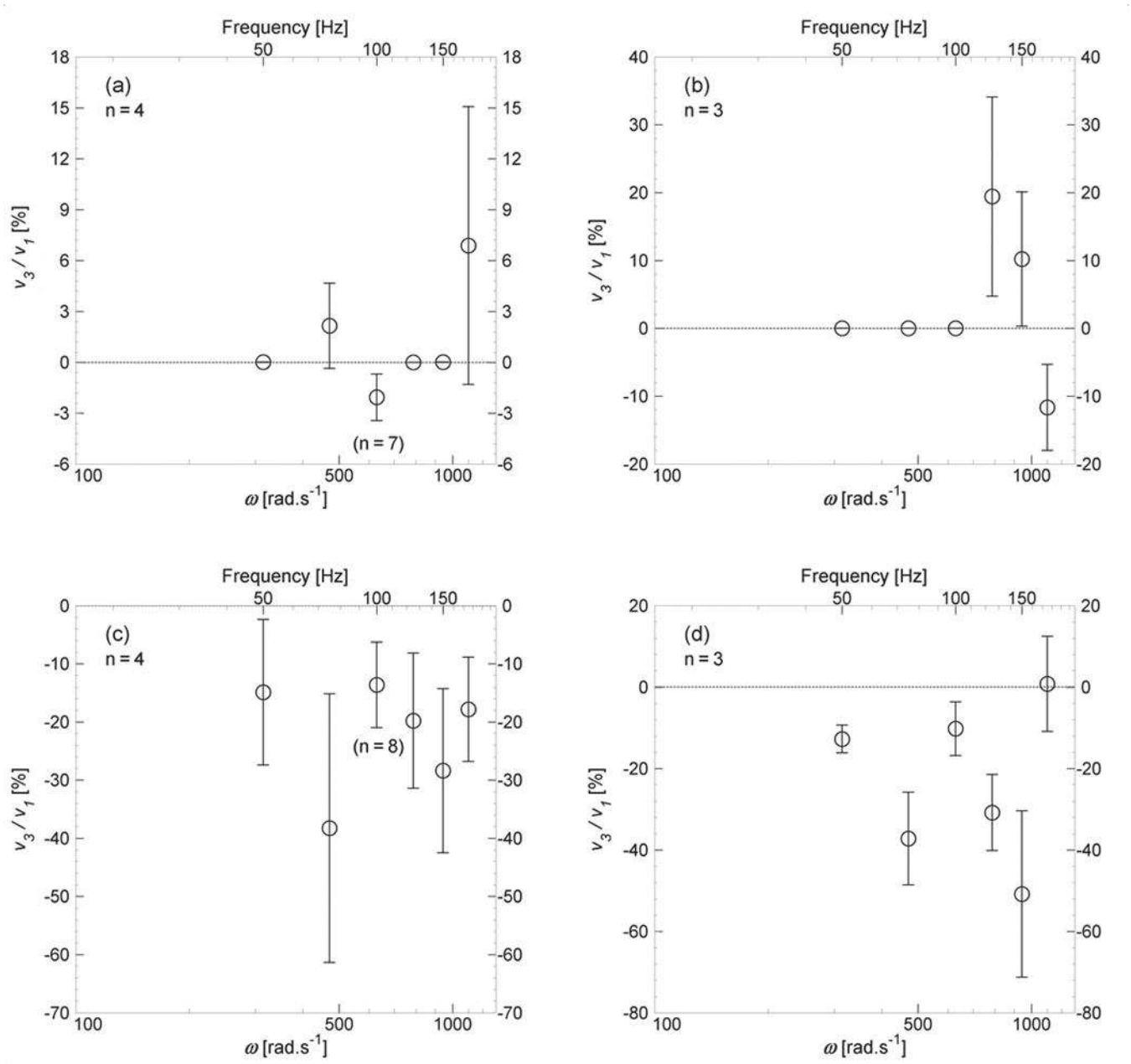

Figure 11.

Intracycle viscous Chebyshev coefficient (v_3/v_1) of vocal fold cover (a, c) and vocal ligament (b, d) as a function of frequency at low strain (1-2%) (a, b) and at high strain (50%) (c, d). Shown are the averages of the viscous Chebyshev coefficient for Subjects 1-8 (sample sizes shown in the upper left corner, except for the vocal fold cover at 100 Hz, where the sample size is indicated in parenthesis).

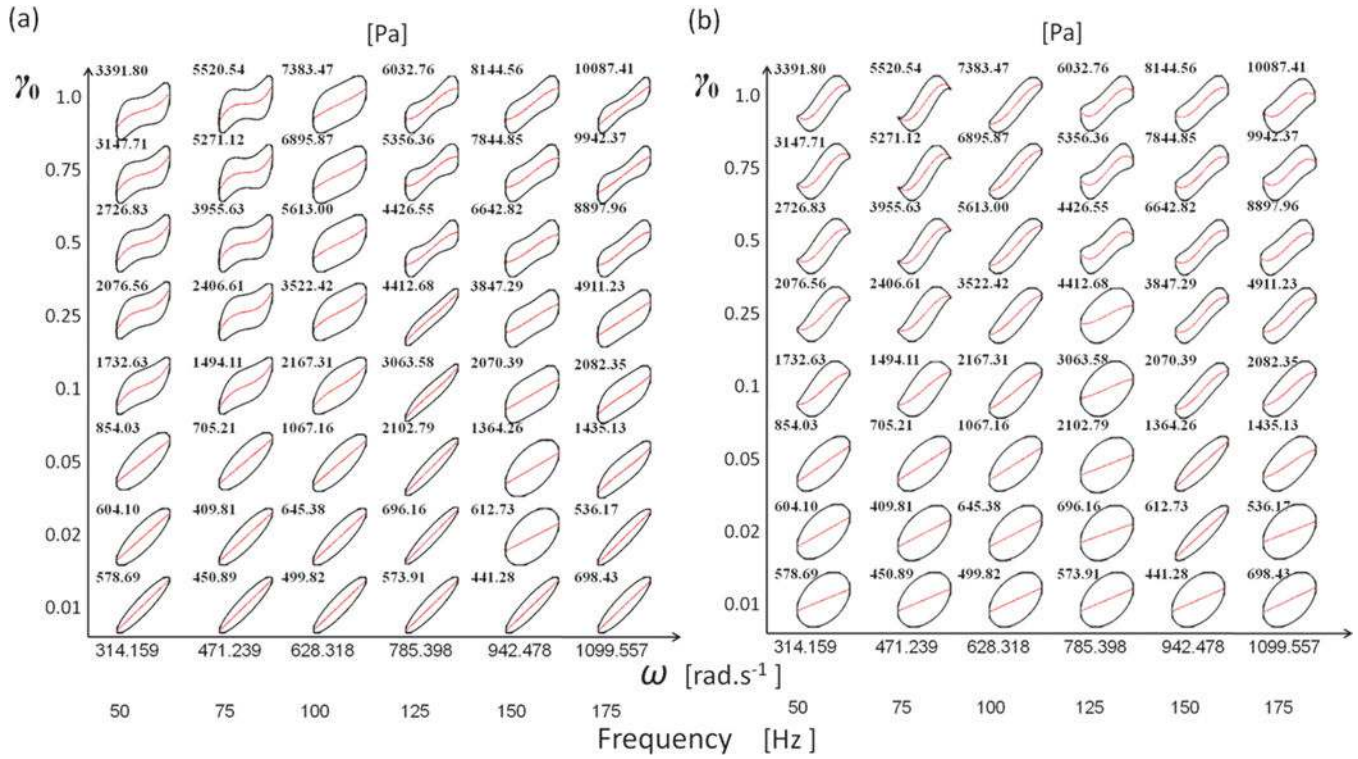

Figure 12.

Smoothed Lissajous-Bowditch curves for the vocal fold cover of a 53-year-old male (Subject 5) displayed in Pipkin space $\{\omega, \gamma_0\}$: (a) elastic curves and (b) viscous curves. The (black) solid lines are the smoothed total stress, and the (red) dashed lines inside are the elastic stress for (a) or the viscous stress for (b). The maximum stress values are indicated above each curve.

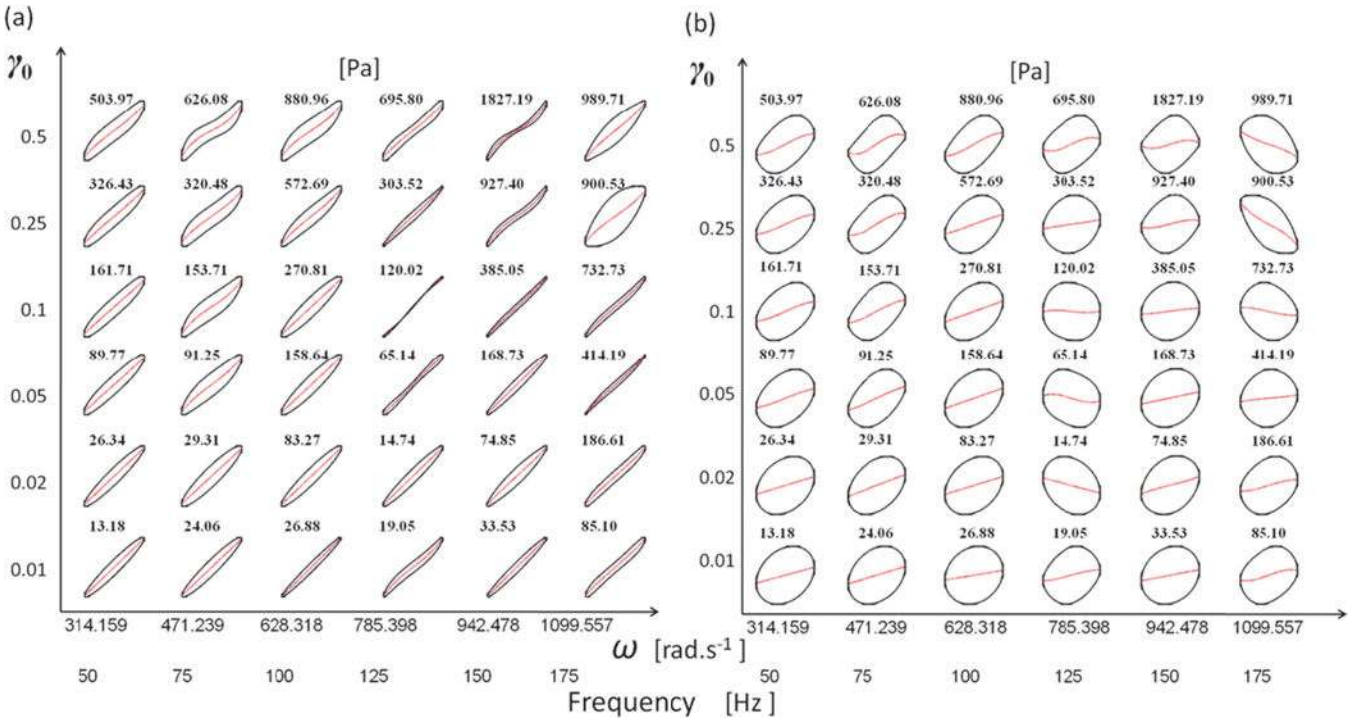

Figure 13.

Smoothed Lissajous-Bowditch curves for the vocal ligament of a 53-year-old male (Subject 5) displayed in Pipkin space $\{\omega, \gamma_0\}$: (a) elastic curves and (b) viscous curves. The (black) solid lines are the smoothed total stress, and the (red) dashed lines inside are the elastic stress for (a) or the viscous stress for (b). The maximum stress values are indicated above each curve.

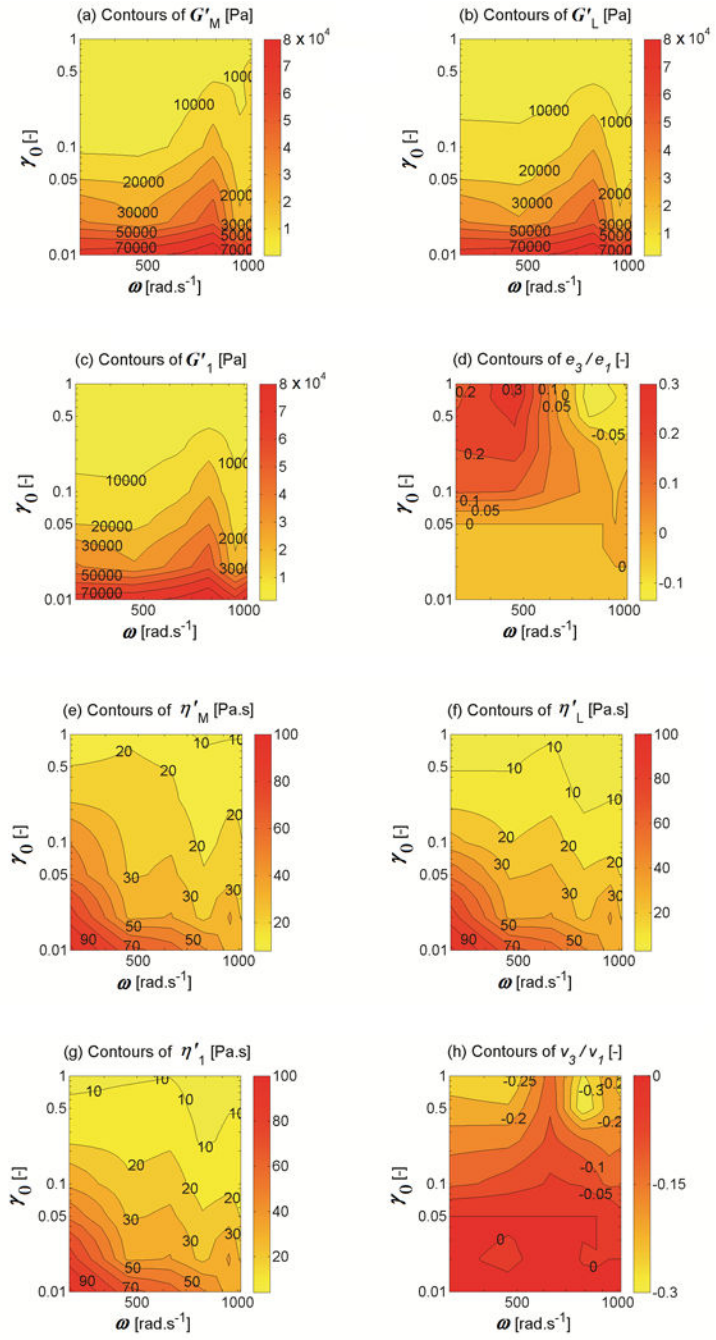

Figure 14.

Rheological fingerprints for the elastic and viscous properties of the vocal fold cover of a 53-year-old male (Subject 5) characterizing the combined effects of ω and γ_0. Elastic measures: (a) G'_M, (b) G'_L, (c) G'_1, and (d) e_3/e_1; viscous measures: (e) η'_M, (f) η'_L, (g) η'_1, and (h) v_3/v_1.

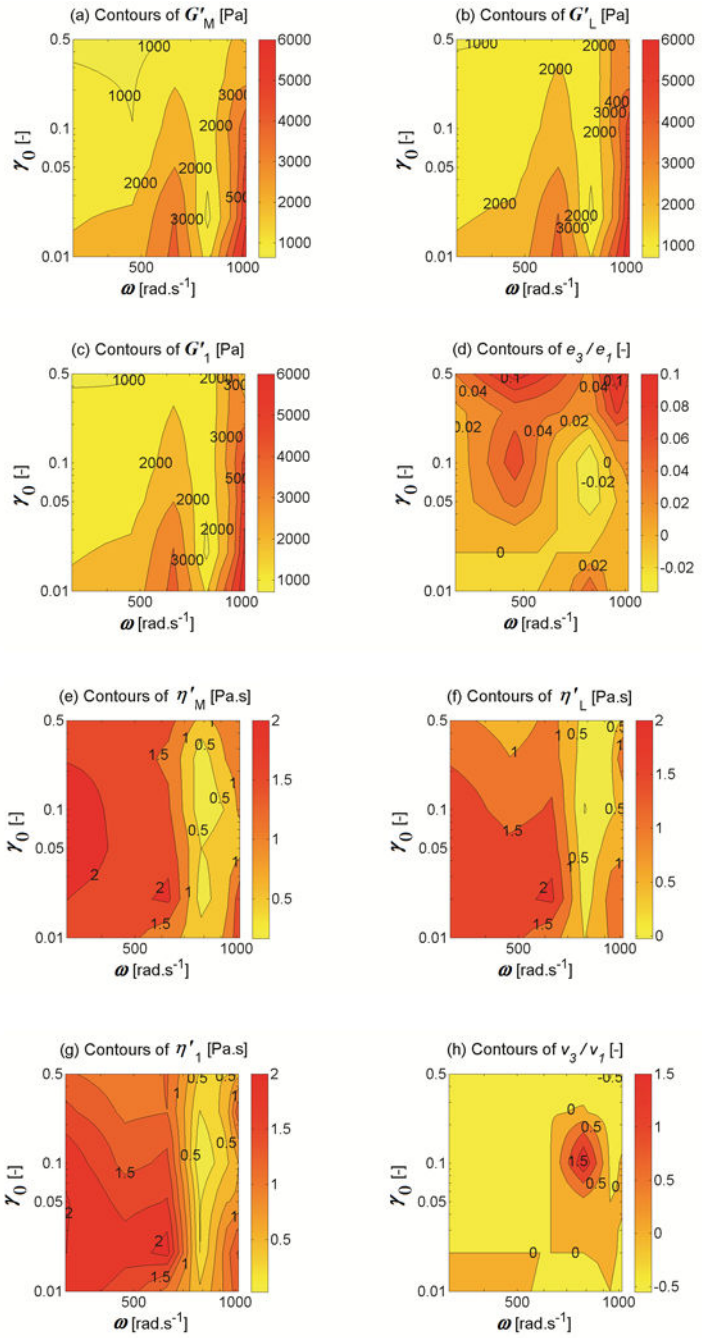

Figure 15.

Rheological fingerprints for the elastic and viscous properties of the vocal ligament of a 53-year-old male (Subject 5) characterizing the combined effects of ω and γ_0. Elastic measures: (a) G'_M, (b) G'_L, (c) G'_1, and (d) e_3/e_1; viscous measures: (e) η'_M, (f) η'_L, (g) η'_1, and (h) v_3/v_1.

Table I

Nomenclature and trends of nonlinear viscoelastic measures for characterizing nonlinear viscoelasticity in response to imposed large-amplitude oscillatory shear (LAOS) deformation, as defined in Ewoldt et al. [8]

Elastic Trends	Indication	Viscous Trends	Indication
G'_M and G'_L decrease with increasing γ_0	Intercycle strain softening	η'_M and η'_L decrease with increasing $\dot{\gamma}_0$	Intercycle shear thinning
G'_M and G'_L increase with increasing γ_0	Intercycle strain stiffening	η'_M and η'_L increase with increasing $\dot{\gamma}_0$	Intercycle shear thickening
If $G'_L > G'_M$ at a single γ_0	Intracycle strain stiffening	If $\eta'_L > \eta'_M$ at a single $\dot{\gamma}_0$	Intracycle shear thickening
If $G'_L < G'_M$ at a single γ_0	Intracycle strain softening	If $\eta'_L < \eta'_M$ at a single $\dot{\gamma}_0$	Intracycle shear thinning
$e_3/e_1 > 0$	Intracycle strain stiffening	$v_3/v_1 > 0$	Intracycle shear thickening
$e_3/e_1 = 0$	Linear elastic behavior	$v_3/v_1 = 0$	Linear viscous behavior
$e_3/e_1 < 0$	Intracycle strain softening	$v_3/v_1 < 0$	Intracycle shear thinning

Table II

Characteristics of the human subjects

Subject	Age	Gender	Ethnicity	Smoking History	Elapsed time (in hours) from tissue procurement to experiment [a]	Vocal fold cover / Vocal ligament
1	60	Male	Caucasian	Nonsmoker	9	Cover
2	88	Male	Caucasian	Nonsmoker	10	Cover
3	53	Female	African American	Nonsmoker	3	Cover
4	58	Female	Hispanic	Nonsmoker	4	Cover
5	53	Male	Caucasian	Nonsmoker	23	Both
6	74	Male	Caucasian	Smoker	1	Cover
7	67	Female	Caucasian	Smoker until 1980s	50	Both
8	76	Female	Caucasian	Smoker until 1970s	39	Both

[a]For subjects 1, 2, 7, 8, it was the number of hours postmortem, i.e., the time that elapsed between a subject's death and the rheometric experiments; For subjects 3 to 6, who were total laryngectomy patients, it was the number of hours elapsed between a subject's surgery and the rheometric experiments.

J Rheol (N Y N Y). Author manuscript; available in PMC 2018 May 18.